Article

Cell Reports

ΔN-Tp63 Mediates Wnt/β-Catenin-Induced Inhibition of Differentiation in Basal Stem Cells of Mucociliary Epithelia

Graphical Abstract

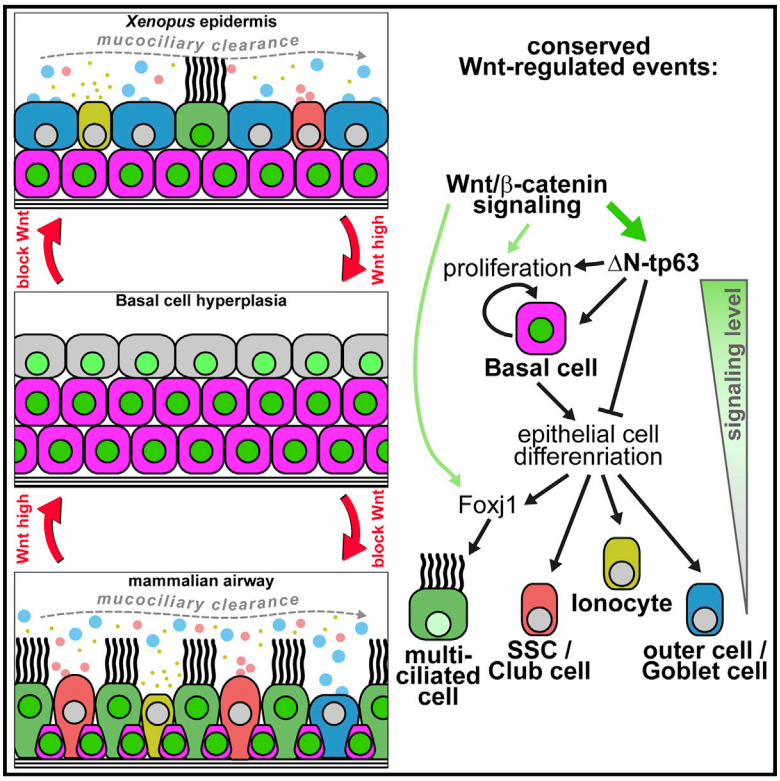

Highlights

- ΔN-TP63 is a master regulator of stemness versus differentiation in mucociliary cells
- Wnt/β-catenin inhibits differentiation by upregulating *ΔN-TP63* in basal stem cells
- Wnt/ΔN-TP63-induced mucociliary remodeling is reversible *in vivo* and *in vitro*
- The *Xenopus* epidermis provides a model to study basal stem cells *in vivo*

Authors

Maximilian Haas,
José Luis Gómez Vázquez,
Dingyuan Iris Sun, ..., Orr Shomroni,
Kris Vleminckx, Peter Walentek

Correspondence

peter.walentek@medizin.uni-freiburg.de

In Brief

Impaired (re-)generation of lung epithelia is associated with Wnt signaling changes in animals and human lung disease patients. Haas et al. demonstrate that ΔN-TP63 is a Wnt-regulated master transcription factor inhibiting (re-) generation of new epithelial cells from stem cells. These findings are equally important for understanding animal development and disease mechanisms.

Haas et al., 2019, Cell Reports *28*, 3338–3352
September 24, 2019
https://doi.org/10.1016/j.celrep.2019.08.063

CellPress

OPEN ACCESS
CellPress

Cell Reports
Article

ΔN-Tp63 Mediates Wnt/β-Catenin-Induced Inhibition of Differentiation in Basal Stem Cells of Mucociliary Epithelia

Maximilian Haas,[1,2,3] José Luis Gómez Vázquez,[1,2,9] Dingyuan Iris Sun,[4,10] Hong Thi Tran,[5] Magdalena Brislinger,[1,2,3,6] Alexia Tasca,[1,2] Orr Shomroni,[7] Kris Vleminckx,[5,8] and Peter Walentek[1,2,3,4,6,11,*]

[1]Internal Medicine IV, Medical Center – University of Freiburg, Faculty of Medicine, University of Freiburg, Freiburg, Germany
[2]Center for Systems Biological Analysis, Albert Ludwigs University Freiburg, Freiburg, Germany
[3]Spemann Graduate School of Biology and Medicine, Albert Ludwigs University Freiburg, Freiburg, Germany
[4]Genetics, Genomics and Development Division, Molecular and Cell Biology Department, University of California, Berkeley, Berkeley, CA, USA
[5]Department of Biomedical Molecular Biology, Ghent University, Ghent, Belgium
[6]CIBSS – Centre for Integrative Biological Signalling Studies, Albert Ludwigs University Freiburg, Freiburg, Germany
[7]Transcriptome and Genome Core Unit, University Medical Center Göttingen, Göttingen, Germany
[8]Department of Biomolecular Medicine, Ghent University, Ghent, Belgium
[9]Present address: Universidad Autónoma de Madrid, Madrid, Spain
[10]Present address: Department of Pathology, University of California, San Francisco, San Francisco, CA, USA
[11]Lead Contact
*Correspondence: peter.walentek@medizin.uni-freiburg.de
https://doi.org/10.1016/j.celrep.2019.08.063

SUMMARY

Mucociliary epithelia provide a first line of defense against pathogens. Impaired regeneration and remodeling of mucociliary epithelia are associated with dysregulated Wnt/β-catenin signaling in chronic airway diseases, but underlying mechanisms remain elusive, and studies yield seemingly contradicting results. Employing the *Xenopus* mucociliary epidermis, the mouse airway, and human airway Basal cells, we characterize the evolutionarily conserved roles of Wnt/β-catenin signaling in vertebrates. In multiciliated cells, Wnt is required for cilia formation during differentiation. In Basal cells, Wnt prevents specification of epithelial cell types by activating *ΔN-TP63*, a master transcription factor, which is necessary and sufficient to mediate the Wnt-induced inhibition of specification and is required to retain Basal cells during development. Chronic Wnt activation leads to remodeling and Basal cell hyperplasia, which are reversible *in vivo* and *in vitro*, suggesting Wnt inhibition as a treatment option in chronic lung diseases. Our work provides important insights into mucociliary signaling, development, and disease.

INTRODUCTION

Mucociliary epithelia line the airways of most vertebrates as well as the epidermis of many vertebrate larvae and invertebrates (Walentek and Quigley, 2017). They are composed of multiple secretory cell types, including Goblet and outer cells, which release mucus, along with Ionocytes, Club cells, and small secretory cells (SSCs), which release ions and small molecules into the extracellular space; in addition, multiciliated cells (MCCs) transport fluid along epithelia by ciliary motion, and Basal cells (BCs) reside underneath the epithelia and serve as tissue-specific stem cells (Hogan et al., 2014; Hong et al., 2004; Rock et al., 2010). Mucociliary epithelia provide a first line of defense against pathogens by mucociliary clearance, which relies on the correct numbers and function of MCCs and secretory cells (Mall, 2008). Aberrations of cell type composition and BC behavior are observed in chronic lung diseases, e.g., chronic obstructive pulmonary disease (COPD), leading to impaired clearance and airway infections (Hogan et al., 2014; Tilley et al., 2015). While chronic lung diseases are among the most common causes of death worldwide, their pathogenic mechanisms are poorly understood and treatment options are limited.

A small number of signaling pathways are employed reiteratively to induce context-dependent responses. This complicates the interpretation of results from experimental manipulations of cell signaling. Wnt/β-catenin signaling regulates gene expression and plays a role in virtually all cells (Clevers, 2006). Signaling is activated by extracellular binding of Wnt ligands to Frizzled receptors and LRP5/6 co-receptors, which then recruit the kinase GSK3β to the membrane, where it is inhibited (Niehrs, 2012). β-catenin is then stabilized and enters the nucleus, where it acts as transcriptional co-regulator through binding to TCF/LEF transcription factors.

Wnt/β-catenin signaling functions in mucociliary epithelia, but results from manipulations often appear contradictory as to the exact roles signaling plays. Wnt/β-catenin was suggested to promote MCC specification and expression of *FOXJ1*, a key transcription factor in motile cilia formation (Brechbuhl et al., 2011; Hou et al., 2019; Huang and Niehrs, 2014; Malleske et al., 2018; Stubbs et al., 2008; Walentek et al., 2012, 2015). In contrast, Wnt/β-catenin activation can also lead to loss of MCCs or Goblet cell hyperplasia (Hashimoto et al., 2012;

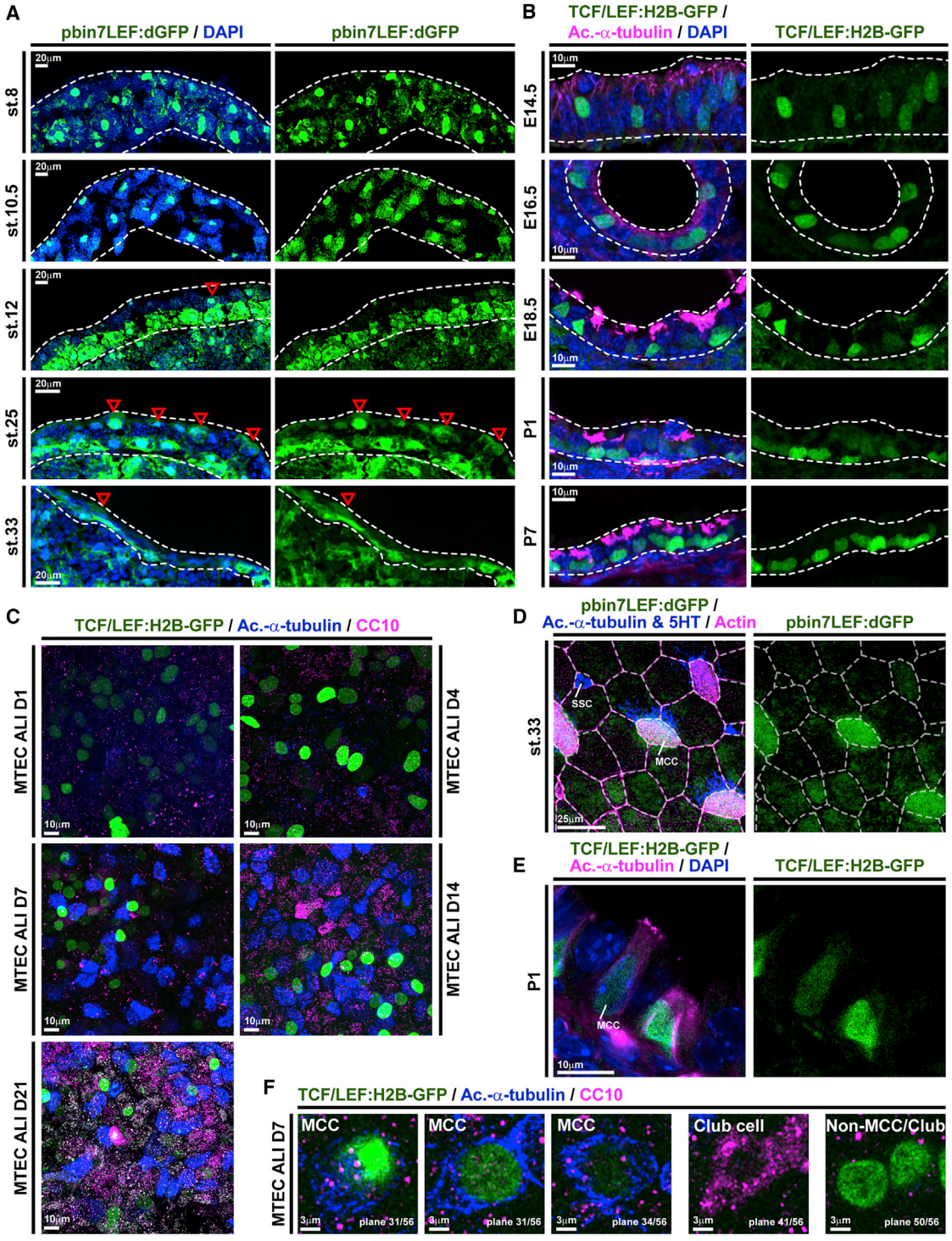

Figure 1. Wnt/β-Catenin Signaling Is Active in MCCs and Basal Progenitors

(A) Analysis of Wnt/β-catenin activity in the *X. laevis* mucociliary epidermis using the pbin7LEF:dGFP reporter line (green). Nuclei are stained by DAPI (blue). Red arrowheads indicate GFP-positive cells in the outer epithelial layer. Dashed lines outline the epidermal layers. Embryonic stages (st. 8–33) are indicated.

(B) Analysis of Wnt/β-catenin activity in the mouse developing airway mucociliary epithelium using the TCF/LEF:H2B-GFP reporter line (green). Nuclei are stained by DAPI (blue) and MCCs are marked by acetylated-α-tubulin (Ac.-α-tubulin, magenta) staining. Dashed lines outline the epithelium. Embryonic (E14.5–18.5) and post-natal (P1–7) stages are indicated.

(legend continued on next page)

Mucenski et al., 2005; Reynolds et al., 2008; Schmid et al., 2017). Additional effects for Wnt were proposed in submucosal glands, during regeneration and in regulating proliferation (Driskell et al., 2004; Hogan et al., 2014; Lynch et al., 2018; Pongracz and Stockley, 2006). Dysregulation of Wnt signaling is commonly observed in chronic lung diseases such as COPD and idiopathic pulmonary fibrosis (IPF) (Baarsma and Königshoff, 2017; Pongracz and Stockley, 2006). Thus, fundamental knowledge on the precise roles of Wnt/β-catenin in mucociliary cells is crucial to understand disease mechanisms and to provide entry points to develop therapies.

We investigated the roles of Wnt/β-catenin in vertebrate mucociliary epithelia using the *Xenopus* epidermis, the mouse airway, and human airway Basal cell culture. Employing a combination of signaling reporters with single-cell resolution, manipulations of the Wnt pathway during various phases of development and regeneration, and epistasis experiments, we characterize the roles of Wnt signaling on mucociliary cell types. Our data confirm a role of Wnt/β-catenin signaling in MCC differentiation but also show its importance in the regulation of BCs. Collectively, we propose that high levels of Wnt/β-catenin signaling block differentiation of BCs into epithelial cell types by activating *ΔN-TP63* expression, which is necessary and sufficient to mediate this effect and to retain stem cells. Importantly, this inhibition of differentiation is reversible *in vivo* and *in vitro*, suggesting local Wnt/β-catenin signaling manipulations to be further explored in the context of chronic lung diseases associated with airway epithelial remodeling.

RESULTS

Wnt/β-Catenin Functions in MCCs and BCs

Wnt signaling was implicated in the specification and differentiation of secretory cells and MCCs in the mammalian airway as well as the *Xenopus* mucociliary epidermis (Huang and Niehrs, 2014; Mucenski et al., 2005; Walentek et al., 2015). To clarify the roles of Wnt/β-catenin signaling in mucociliary cell types, we analyzed signaling activity using transgenic reporter lines expressing GFP upon Wnt/β-catenin activation in *Xenopus* and the mouse (Borday et al., 2018; Ferrer-Vaquer et al., 2010). Wnt activity was assessed throughout development of the *Xenopus* epidermis and in the mouse conducting airways (Figure 1; Figure S1). While the epidermis and the airways are derived from different germ layers and formed at different stages relative to organismal development (Walentek and Quigley, 2017; Warburton et al., 2010), our analysis revealed striking similarities in Wnt activity in both tissues. Initially, signaling was observed in cells throughout the epithelia, without particular compartmentalization. With progressive development, Wnt activity was restricted to the sensorial layer of the *Xenopus* epidermis (Figure 1A) and the basal compartment of the airway epithelium (Figure 1B). In both systems, the location of Wnt-positive cells coincided with the known location of the respective progenitor cell population that gives rise to MCCs and secretory cells, which then intercalate into the epithelium during differentiation (Deblandre et al., 1999; Rock et al., 2009; Stubbs et al., 2006). In *Xenopus*, we also observed GFP-positive cells in the epithelial cell layer during intercalation stages (stage [st.] 25) (Figure 1A, arrowheads). En-face imaging after immunostaining for cell type markers revealed increased Wnt activity in intercalating MCCs and Ionocytes at st. 25 (Figure S1C). In the mature mucociliary epidermis, Wnt activity was then restricted to MCCs (Figure 1D). We also detected elevated Wnt activity in differentiating MCCs of the mouse airway, although reporter activity was lower in MCCs as compared to cells residing at the base of the epithelium (Figure 1E; Figure S1D). We generated mouse tracheal epithelial cell (MTEC) cultures from Wnt reporter animals and monitored Wnt activity in the air-liquid interface (ALI) *in vitro* model at days 1, 4, 7, 14, and 21 (Vladar and Brody, 2013). Wnt activity was detected throughout all stages of regeneration, with MCCs showing elevated signaling levels as well as reporter-positive cells residing basally, but no Wnt activity was detected in Club cells (Figures 1C and 1F; Figure S1E).

These data suggested a role for Wnt/β-catenin in basal progenitor cells as well as in MCCs. To test this, we knocked down β-catenin using morpholino-oligonucleotide (MO) injections targeting the *Xenopus* epidermis and analyzed epidermal morphology as well as MCCs (Figure 2A). We observed increased numbers of MCCs in *β-catenin* morphants (*β-catenin* MO), but these MCCs presented reduced cilia numbers (Figures 2A and 2B). These data resembled experiments using overexpression of *dickkopf 1* (*dkk1*) in *Xenopus* (Walentek et al., 2015). Reduced ciliation rate in β-catenin-deficient MCCs was also compatible with data demonstrating that β-catenin is a transcriptional co-regulator of *foxj1*, which is required for motile ciliogenesis in MCCs (Caron et al., 2012; Gomperts et al., 2004; Stubbs et al., 2008; Walentek et al., 2012). Nevertheless, the question arose as to why reduced β-catenin levels increased the overall number of MCCs in the epithelium. As the basal precursor cell compartment was the site of highest Wnt signaling reporter activity in both *Xenopus* and mice, we wondered if loss of β-catenin would affect BCs and lead to increased MCC specification. We injected *β-catenin* MO targeting exclusively the right side of embryos and analyzed marker gene expression for MCCs and BCs at mid-neurula stages (st. 17), i.e., after cell fate specification. *In situ* hybridization (ISH)

(C) MTEC ALI cultures generated from the TCF/LEF:H2B-GFP reporter line (green) and cultured up to 21 days (D21) revealed Wnt signaling activity throughout the different stages. n = 3 cultures per time point. MTECs were stained for Ac.-α-tubulin (blue) and CC10 (magenta). Only primary cilia were present at days 1 and 4 (D1 and 4), and MCCs could be detected from day 7 (D7) onward.

(D) En-face imaging of the mature *Xenopus* epidermis at st. 33 shows elevated signaling levels (green) in MCCs (Ac.-α-tubulin, blue). SSCs (5HT, blue). Cell membranes are visualized by actin staining (magenta).

(E) Immunostaining for Ac.-α-tubulin (magenta) and nuclei (DAPI, blue) shows high levels of Wnt signaling (green) in cells with BC morphology and intermediate signaling levels in differentiating MCCs.

(F) Single confocal sections of MTECs at ALI day 7 (D7) show MCCs (Ac.-α-tubulin, blue) with variably elevated signaling levels (green), Club cells (CC10, magenta) without Wnt activity, and non-MCC/non-Club cells with elevated Wnt signaling levels at the base.

Related to Figure S1.

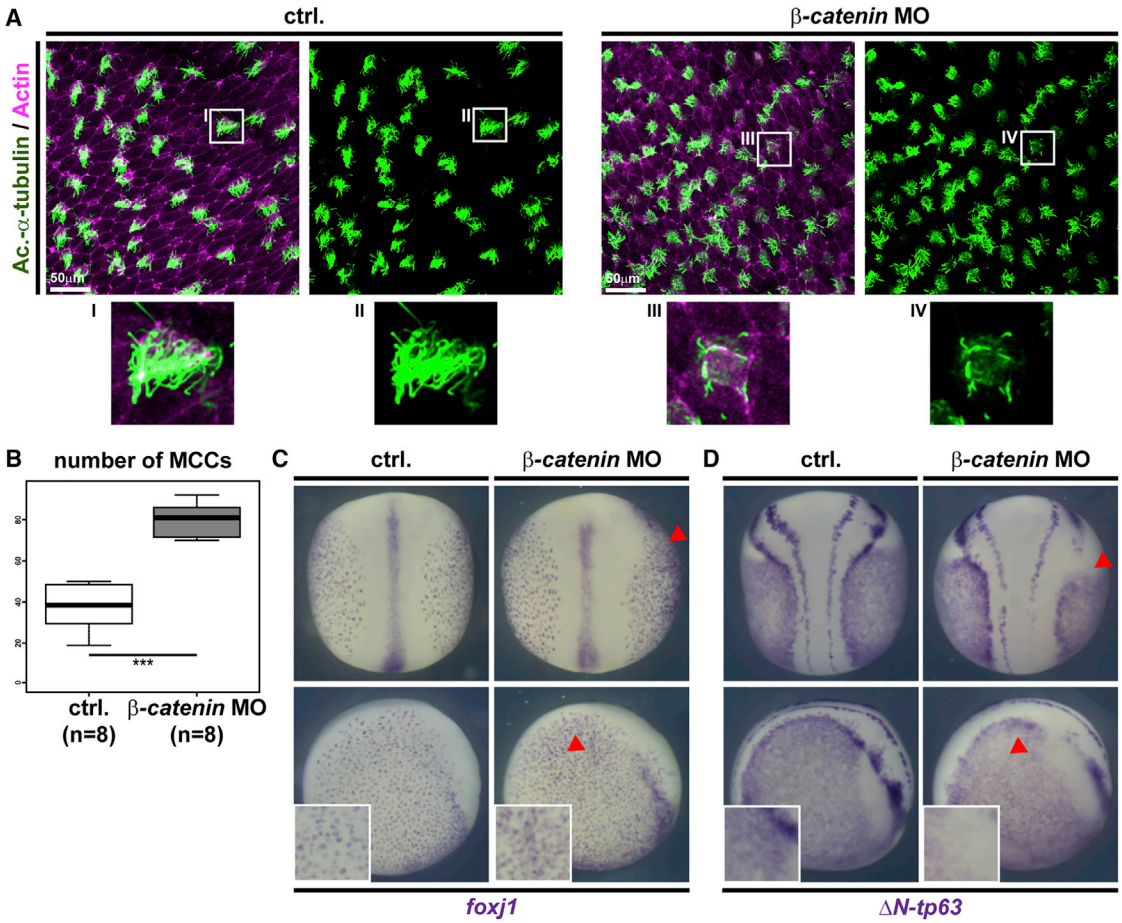

Figure 2. Wnt/β-Catenin Regulates MCC Numbers and *ΔN-tp63* Expression

(A) Morpholino-oligonucleotide (MO) knockdown of *β-catenin* in *Xenopus* increases MCC numbers (Ac.-α-tubulin, green), but MCCs present fewer and shorter cilia than controls (ctrl.). Actin staining (magenta). Insets indicate locations of magnified areas I–IV.

(B) Quantification of results depicted in (A). Mann Whitney test, *** $p \leq 0.001$.

(C) ISH reveals increased MCC numbers (*foxj+* cells) after unilateral knockdown of β-catenin (*β-catenin* MO). Controls (n = 13); *β-catenin* MO (n = 22).

(D) ISH reveals decreased *ΔN-tp63* expression after *β-catenin* MO. Controls (n = 27); *β-catenin* MO (n = 37).

In (B) and (C), the injected side is indicated by red arrowheads. Dorsal views are shown in upper panels, lateral views are shown in the lower panels, and magnified views are depicted in white boxes.

for *foxj1* (MCCs) and *ΔN-tp63* (sensorial layer BCs; Cibois et al., 2015; Lu et al., 2001) revealed an increase in *foxj1*-positive cells and reduced *ΔN-tp63* expression on the injected side of the embryos (Figures 2C and 2D). This implicated an increase in MCC specification at the expense of basal progenitors upon Wnt inhibition. Collectively, our experiments identified MCCs and BCs as sites of elevated signaling activity during mucociliary development and a requirement for controlled Wnt/β-catenin signaling in MCCs and BCs to generate a normal mucociliary epithelium.

ΔN-Tp63 Is Necessary and Sufficient to Block Differentiation in Response to Wnt/β-Catenin

Airway BCs are tissue-specific stem cells and required for maintenance and regeneration of all mucociliary cell types (Rock et al., 2010; Zuo et al., 2015). *ΔN-TP63-α/β* are the dominantly expressed isoforms of the transcription factor TP63 in airway BCs and a commonly used marker for BCs in various epithelia (Arason et al., 2014; Soares and Zhou, 2018; Warner et al., 2013). Expression of *ΔN-TP63* isoforms is regulated by an evolutionarily conserved alternative promotor (P2) initiating transcription at alternative exon 3 (Ruptier et al., 2011). In *Xenopus*, only *ΔN-tp63* isoforms are expressed during development, and no full-length isoform is annotated in the *X. laevis* or *X. tropicalis* genomes to date, indicating potential loss of this isoform in the frog. Nevertheless, in *Xenopus* and in mammals, chromatin immunoprecipitation and DNA sequencing (chromatin immunoprecipitation sequencing [ChIP-seq]) has detected multiple TCF/LEF binding sites in P2, suggesting direct Wnt/β-catenin regulation (Kjolby and Harland, 2017; Ruptier et al., 2011). Since *ΔN-TP63* is associated with the regulation of differentiation and given our observation that loss of β-catenin lead to decreased *ΔN-tp63* expression, we tested if *ΔN-tp63* was Wnt regulated in the mucociliary epidermis. Ectopic activation of Wnt/β-catenin signaling was achieved by application of the

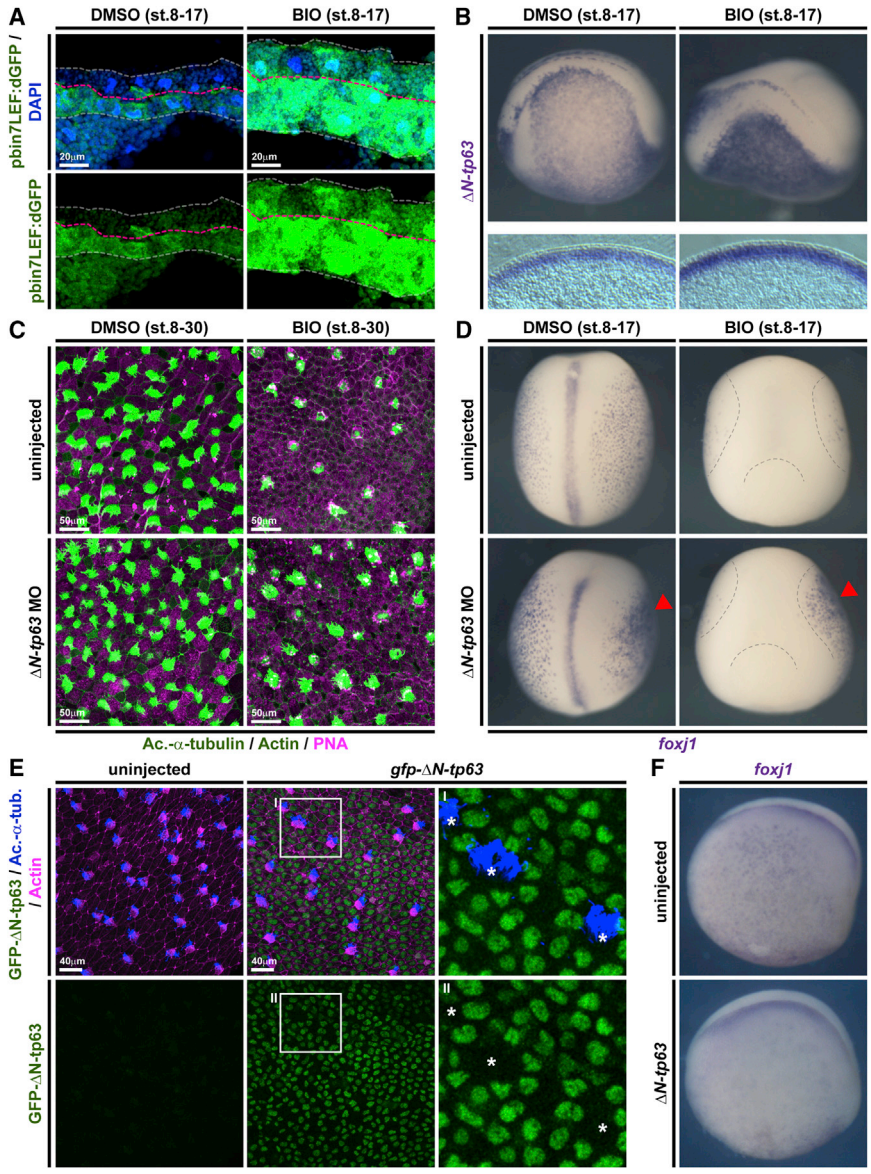

Figure 3. ΔN-tp63 Mediates Wnt/β-Catenin-Induced Inhibition of Cell Fate Specification in *Xenopus*

(A–D) BIO treatments from st. 8–17 or st. 8–30. DMSO was used as vehicle control.

(A) Confocal imaging shows Wnt/β-catenin signaling activation (green) and thickening of the epidermis in BIO-treated embryos. Nuclei (DAPI, blue). DMSO (n = 2); BIO (n = 2).

(B) *In situ* hybridization (ISH) shows increased intensity and thickness of the ΔN-tp63 expression domain in BIO-treated whole mounts (upper row) and transversal sections (bottom row).

(C) BIO treatment reduces MCC (Ac.-α-tubulin, green), Ionocyte (no staining, black), and SSC (large vesicles, peanut agglutinin [PNA] staining, magenta) numbers in confocal micrographs. Actin staining (green). *ΔN-tp63* MO in controls leads to increased MCCs and Ionocytes, while *ΔN-tp63* MO in BIO-treated embryos rescues MCC and Ionocyte formation.

(D) ISH reveals reduced MCC numbers (*foxj+* cells) after BIO treatment, while unilateral knockdown of *ΔN-tp63* in control treated embryos leads to more *foxj+* cells and rescues *foxj+* cell numbers in BIO-treated embryos. DMSO (n = 5); BIO (n = 7); DMSO+*ΔN-tp63* MO (n = 5); BIO+*ΔN-tp63* MO (n = 4). Injected side is indicated by red arrowhead. Dashed lines indicate epidermal area in BIO-treated embryos.

(E) Overexpression of *gfp-ΔN-tp63* mRNA leads to nuclear localization of the protein (green) and reduced MCC (Ac.-α-tubulin, blue) numbers at st. 30. Actin staining (magenta). Differentiated MCCs in injected specimens show no nuclear GFP signal (asterisks), indicating that they were not targeted. Magnified areas I–II are indicated.

(F) ISH for *foxj1* at st. 17 shows reduced MCCs in *ΔN-tp63* mRNA injected embryos.

Related to Figures S2 and S3.

GSK3β-inhibitor 6-Bromoindirubin-3′-oxime (BIO) to the medium starting at st. 8 of *Xenopus* development. Efficient activation of the Wnt pathway in the epidermis was confirmed using the Wnt reporter line (Figure 3A). First, we analyzed the effects of BIO treatment on epidermal *ΔN-tp63* expression by ISH. Specimens treated with BIO displayed increased levels of *ΔN-tp63* expression and a thickening of the sensorial layer (Figure 3B; Figure S2A). Next, we treated embryos with BIO from st. 8 until st. 30, when MCCs and Ionocytes have fully developed, and analyzed cell type composition by immunofluorescent staining (Walentek, 2018). Treatment with BIO significantly reduced the numbers of all intercalating cell types in a dose-dependent manner (Figure 3C; Figures S2B and S2C). Lack of mature MCCs and Ionocytes could be a result of inhibited cell fate specification or defective differentiation and intercalation into the epithelium. Therefore, we also tested the effects of BIO treatment on the expression of early cell-type-markers associated with successful cell fate specification by ISH at st. 17, i.e., before intercalation (Walentek and Quigley, 2017). We observed a loss or strong reduction in cell-type-marker expression for MCCs (*foxj1*), Ionocytes (*foxi1*; Quigley et al., 2011), and SSCs (*foxa1*; Dubaissi et al., 2014), indicating a failure in cell fate specification after BIO application (Figure 3D; Figures S2D and S2E). These data suggested that increased Wnt/β-catenin lead to upregulation of *ΔN-tp63* and expansion of the BC pool, while inhibiting specification of epidermal cell types. To directly test if ΔN-tp63 was necessary for the block of specification in response to Wnt overactivation, we injected embryos with a *ΔN-tp63* MO at four-cell stage and treated the morphants either with vehicle or BIO, starting at st. 8. Cell type quantification at st. 30 and ISH marker analysis at st. 17 both showed a partial rescue of cell fate specification and morphogenesis in *ΔN-tp63* MO embryos treated with BIO and an increased specification of MCCs and Ionocytes in *ΔN-tp63* MO morphants without BIO

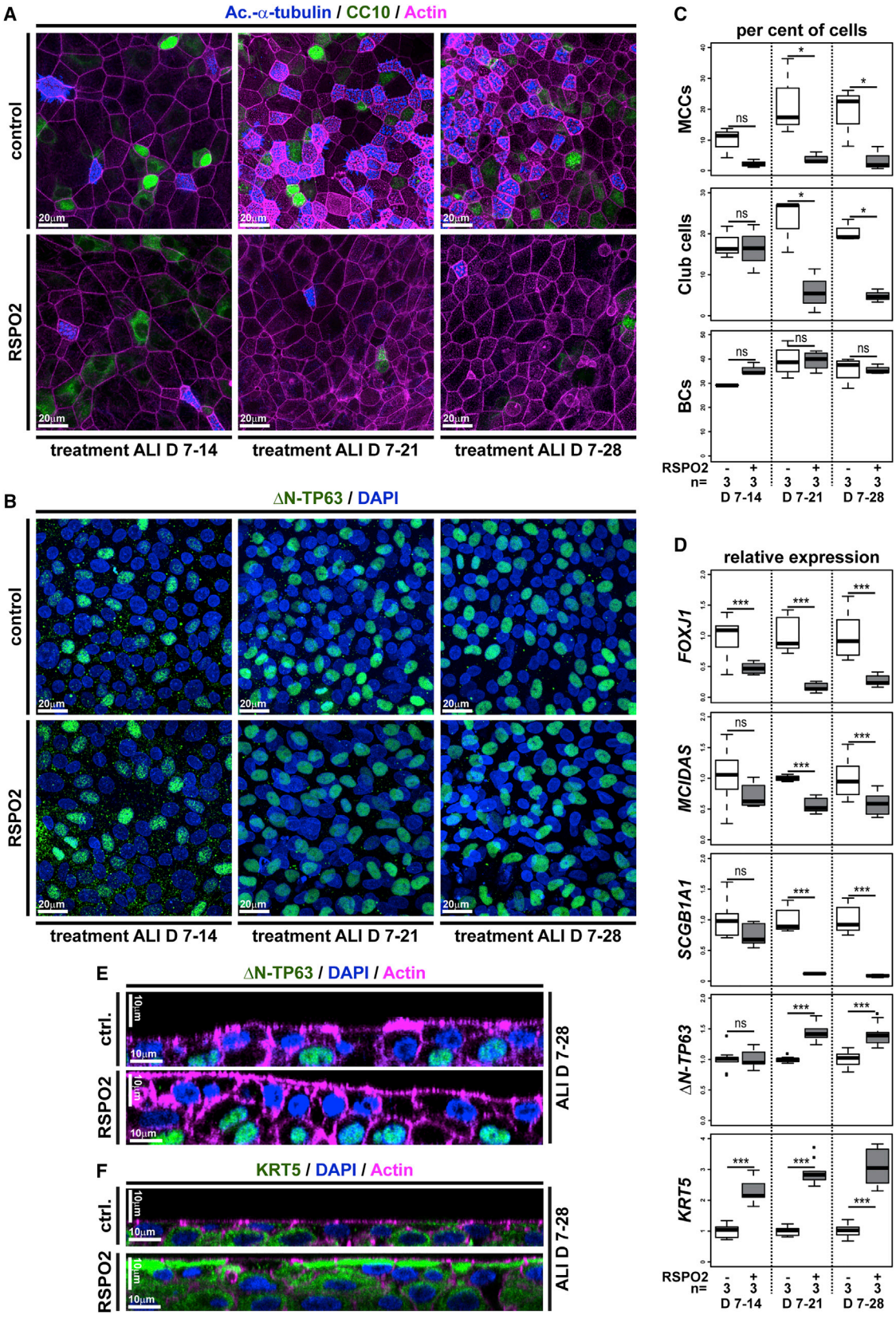

(legend on next page)

application (Figures 3C and 3D; Figures S2B–S2E). Together, these results indicated that *ΔN-tp63* activation was necessary to block differentiation upon BIO treatment. Next, we wondered if ΔN-tp63 alone was sufficient to inhibit differentiation in the absence of increased Wnt signaling. Therefore, we generated GFP-tagged and untagged ΔN-tp63 constructs. Overexpression of *gfp-ΔN-tp63* in the epidermis and immunofluorescent staining confirmed successful production of the protein and its nuclear localization (Figure 3E). Furthermore, injections of *gfp-ΔN-tp63* or *ΔN-tp63* reduced MCC numbers and expression of early cell type markers for MCCs, Ionocytes, and SSCs (Figures 3E and 3F; Figures S3A–S3C), thereby providing evidence for sufficiency. Additionally, we investigated if ΔN-tp63 only inhibits cell fate specification from BCs or if its activity in cells after specification could inhibit differentiation as well. For that, we generated a hormone-inducible version of GFP-ΔN-tp63 (GFP-ΔN-tp63-GR; Kolm and Sive, 1995), injected embryos at four-cell stage, and added dexamethasone (Dex) to the medium at various stages of development. Activation of the construct and subsequent nuclear localization was confirmed by confocal microscopy (Figure S3D). Dex addition at st. 9 suppressed MCC formation as observed with the non-inducible construct, whereas application of vehicle at st. 9 or Dex activation after MCC specification at st. 24 did not result in reduced MCC numbers at st. 30 (Figures S3E and S3F). High-magnification imaging further confirmed presence of GFP-ΔN-tp63-GR in the nuclei of fully differentiated MCCs and Ionocytes in specimens activated at st. 24 (Figure S3G). These results indicated that the inhibitory effect of ΔN-tp63 on epithelial cell specification was restricted to basal progenitors. Finally, we investigated the degree of evolutionary conservation of the observed effects in human airway basal stem cells. Ectopic activation of canonical Wnt signaling in ALI cultures derived from immortalized human airway BCs (BCi-NS1.1 cells [BCIs]; Walters et al., 2013) was induced by application of human recombinant R-spondin 2 (RSPO2) protein to the medium after initial epithelialization of cultures was completed at ALI day 7. We then analyzed the effects of RSPO2 on airway mucociliary regeneration by immunofluorescent staining and quantitative real-time PCR. In BCIs, RSPO2 application inhibited differentiation of MCCs and Club secretory cells (Figures 4A, 4C, and 4D). At the same time, we observed an increase in *ΔN-TP63* expression after RSPO2 treatment as well as elevated levels for *KRT5* (*Keratin 5*), an additional marker for BCs in airway epithelia (Figures 4C–4E) (Zuo et al., 2015). Orthogonal optical sections of confocal images from BCIs stained for ΔN-TP63 or KRT5 further revealed an increase in epithelial thickness and epithelial KRT5-positive cells after RSPO2 treatment (Figures 4E and 4F; Figures S4A and S4B), similar to our observations in *Xenopus* and reminiscent of phenotypes in COPD patients (Rock et al., 2010), potentially indicating early BC hyperplasia. This interpretation of results was further supported by quantification of Ki67-positive proliferative cells, which increased in number upon RSPO2 treatment, while the total number of epithelial cells remained low, likely due to inhibited specification and intercalation of MCCs and Club cells into the epithelium (Figures S4C–S4E). To address if Goblet cell hyperplasia occurred after Wnt/β-catenin gain of function in addition to effects on MCC and Club cell specification, we also analyzed mucin expression. Quantitative real-time PCR on BCIs treated with RSPO2 revealed reduced *MUC5A/C* expression, while the expression of *MUC5B* was elevated (Figures S4F and S4G). Nevertheless, immunofluorescent staining did not detect an increase in epithelial cells staining for MUC5B (Figure S4H). In summary, our data revealed that ΔN-TP63 was necessary and sufficient to inhibit differentiation of mucociliary epithelial cell types from BCs in response to canonical Wnt activation, without the need for Goblet cell hyperplasia. Furthermore, our results suggested that prolonged overactivation of Wnt signaling could lead to BC hyperplasia and long-term remodeling of the airway epithelium.

ΔN-Tp63 and Wnt Signaling Are Required for Maintenance of BCs and Correct Cell Type Composition in Mucociliary Epithelia

While our results argued for an important role for ΔN-TP63 in BCs of mucociliary epithelia, we found it astonishing that developmental loss of ΔN-TP63 in mammals (Daniely et al., 2004) and *Xenopus* (this study) still allowed for the formation of a mucociliary epithelium. We therefore tested how *ΔN-tp63* knockdown affected the mucociliary epidermis in more detail. In contrast to MCCs and Ionocytes, which intercalate early (st. 25) and are fully mature by st. 30, SSCs appear and mature slightly later (Walentek et al., 2014), resulting in approximately equal numbers of MCCs, Ionocytes, and SSCs in the mucociliary epidermis by st. 34 (Figure 5C) (Walentek, 2018). Injections of *ΔN-tp63* MO and subsequent analysis of cell type composition at st. 34 revealed a moderate increase in MCCs and Ionocytes but a significant decrease in SSCs (Figures 5A, 5C, and 5D). These results suggested that premature release of BCs into differentiation could have reduced the availability of BCs during later stages of SSC specification. Therefore, we tested if SSCs are indeed specified after MCCs and Ionocytes or if their late appearance in the epithelium could be a consequence of

Figure 4. Wnt/β-Catenin Signaling Inhibits Differentiation and Promotes Stemness in Human BCs

(A–F) Human immortalized BC (BCIs) kept in air-liquid interface (ALI) culture for up to 4 weeks. Human recombinant R-spondin2 (RSPO2) was used to activate Wnt/β-catenin signaling starting at ALI day 7 (D7). n = 3 cultures per time point and treatment.

(A) Confocal imaging of specimens stained for Ac.-α-tubulin (MCCs, blue), CC10 (Club cells, green), and Actin (cell membranes, magenta) show reduced MCC and Club cell numbers in RSPO2-treated cultures.

(B) RSPO2 does not reduce the number of ΔN-TP63+ (green) cells. Nuclei (DAPI, blue).

(C) Quantification from (A) and (B). Mann Whitney test, not significant, ns ($p > 0.05$); *$p \leq 0.05$; **$p \leq 0.01$; ***$p \leq 0.001$.

(D) Quantitative real-time PCR. Expression levels are depicted relative to stage controls. RSPO2 reduces expression of MCC (*FOXJ1*, *MCIDAS*) and Club cell (*SCGB1A1*) markers but increases expression of BC markers (*ΔN-TP63*, *KRT5*). Student's t test, not significant, ns ($p > 0.05$); *$p \leq 0.05$; **$p \leq 0.01$; ***$p \leq 0.001$.

(E and F) Optical orthogonal sections of confocal images. RSPO2-treated cultures display increased epithelial thickness and cells staining for BC markers ΔN-TP63 (green, in E) and KRT5 (green, in F).

Related to Figure S4.

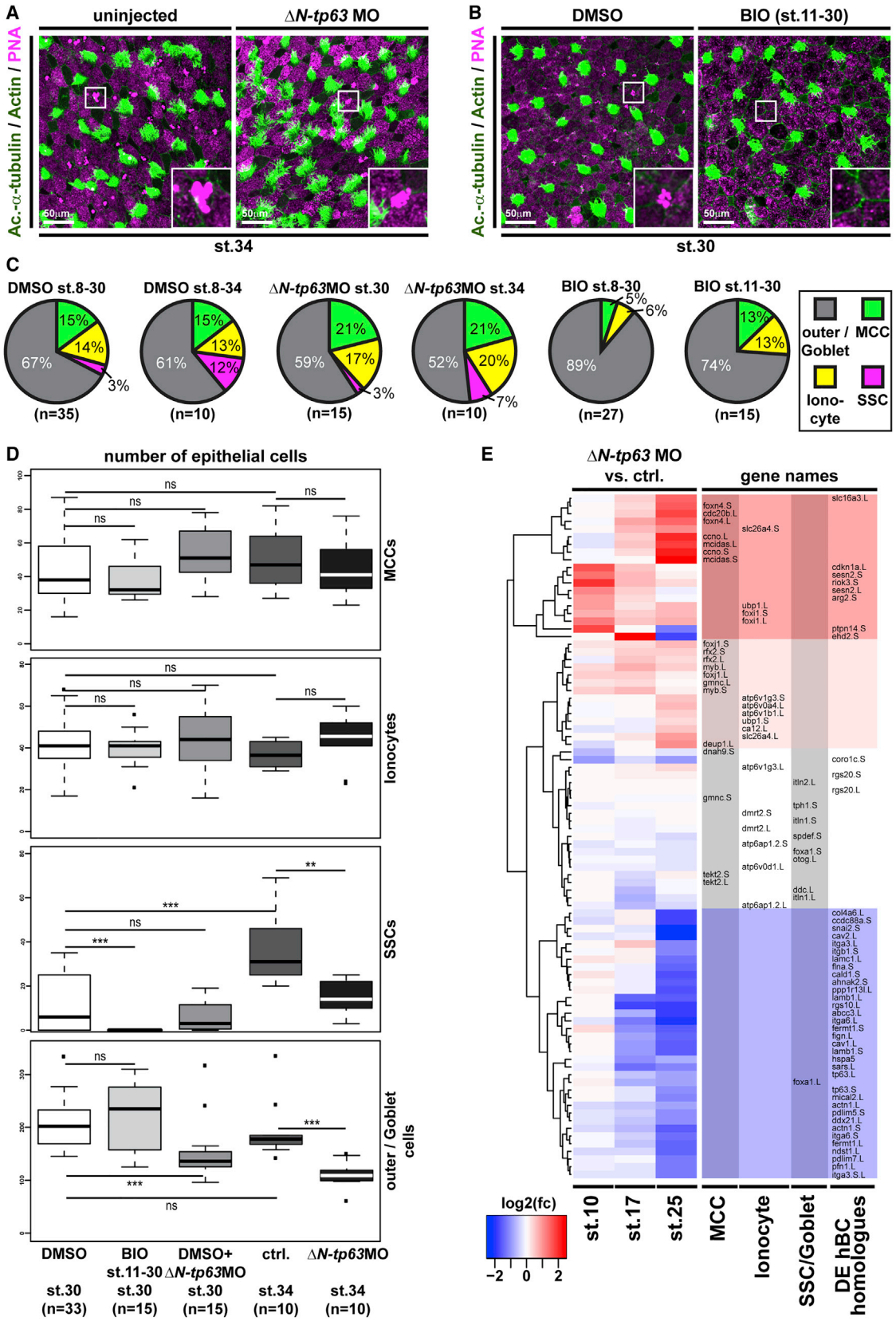

(legend on next page)

prolonged differentiation or slower intercalation. For that, embryos were treated with BIO, starting at st. 11. This later stimulation of Wnt/β-catenin signaling resulted in almost normal MCC and Ionocyte numbers but completely inhibited the appearance of SSCs (Figures 5B–5D). These data strongly indicated that SSCs were derived from the same BC progenitor pool during development as MCCs and Ionocytes and that SSCs were specified later. To test if *Xenopus* BCs were lost by *ΔN-tp63* MO, we generated mucociliary organoids from *Xenopus* animal cap explants, providing pure mucociliary tissue for RNA sequencing (RNA-seq) (Walentek and Quigley, 2017). Organoids were generated from control and *ΔN-tp63* morphant embryos and collected for total RNA extraction at early (st. 10) and late (st. 17) cell-fate-specification stages as well as after specification was completed (st. 25). RNA-seq and differential expression analysis revealed significant differences in gene expression between control and *ΔN-tp63* morphant samples, and the most differentially expressed genes were detected at st. 25 (243 genes with P-adj < 0.05; Figure S5A; Table S1) (Love et al., 2014). Among significantly upregulated genes, we found MCC and Ionocyte genes, including *mcidas*, *ccno*, *cdc20b*, *foxn4*, and *foxi1*, and Gene Ontology (GO)-term analysis indicated enrichment for "multi-ciliated epithelial cell differentiation" (Table S1; Figure S5B) (Mi et al., 2013; Walentek and Quigley, 2017). In contrast, GO-term analysis of significantly downregulated genes identified an enrichment for the terms "focal adhesion," "actin cytoskeleton," and "extracellular matrix" (Figure S5B). These terms were also found to be enriched within the human airway BC transcriptome, suggesting loss of BCs (Hackett et al., 2011). Next, we compared the list of differentially expressed genes in *ΔN-tp63* morphants with the human airway BC transcriptome and identified 41 dysregulated *Xenopus* homologs, including multiple regulators of proliferation and of cell and extracellular matrix interactions (Figure 5E). We subjected their relative expression values, as well as those of *ΔN-tp63* (log2 fold change relative to controls), to hierarchical clustering. In our analysis, we also included a subset of previously identified *Xenopus* core MCC and Ionocyte markers as well as known markers for SSCs and Goblet (outer-layer) cells (Dubaissi et al., 2014; Hayes et al., 2007; Quigley and Kintner, 2017). The two clusters representing the most upregulated genes over developmental time in *ΔN-tp63* morphants contained key markers for MCCs (e.g., *mcidas*, *ccno*, *cdc20b*, *foxj1*, *myb*) and Ionocytes (e.g., *foxi1*, *atp6* subunits, *ca12*, *ubp1*) (Figure 5E). In contrast, the cluster representing the most downregulated genes over developmental time contained exclusively BC markers (e.g., *ΔN-tp63*, *itga3/6*, *itgb1*, *lamb1*, *cav2*) and the key transcription factor for SSC specification *foxa1* (Figure 5E). Together, these data not only revealed a high degree of functional and transcriptional homology between human and *Xenopus* mucociliary BCs but also demonstrated that ΔN-tp63 was necessary for the maintenance of BCs during development, which was in turn required to generate a normal cell type composition in the mucociliary epidermis. Furthermore, these data were in line with previous work, demonstrating that loss of ΔN-TP63 impaired regeneration and induced senescence in human ALI cultures (Arason et al., 2014). Therefore, we wondered if elevated Wnt/β-catenin signaling in the airway basal compartment was required for the maintenance *ΔN-TP63* expression and BCs in human cells after epithelialization as well. To test this, we inhibited Wnt/β-catenin signaling by addition of human recombinant DKK1 protein (DKK1) to the medium of differentiating BCI ALI cultures starting at ALI day 7. Quantification of cell type markers and mRNA expression levels by immunofluorescence and quantitative real-time PCR showed a moderate increase in MCCs and Club cells and a relative decrease in BCs in DKK1-treated cultures but not a long-term loss of BCs (Figures 6A–6F). Furthermore, proliferation and the total number of epithelial cells remained unchanged, and Mucin production was not inhibited after DKK1 treatment (Figures S5C–S5H). These data indicated that Wnt/β-catenin regulated the decision between BC identity and differentiation into epithelial cell types but that it was dispensable in later phases of *in vitro* regeneration for maintenance of *ΔN-TP63* expression and BCs. In summary, our experiments demonstrated that ΔN-TP63 was a master transcription factor in BCs regulating the decision between differentiation and basal stem cell fate in vertebrate mucociliary epithelia and that Wnt/β-catenin was required for maintaining *ΔN-TP63* expression and BCs during development but not in later phases of regeneration.

Wnt/β-Catenin-Induced Block of Differentiation Is Reversible

Given the importance of correctly regulated Wnt/β-catenin signaling for BCs as well as for the generation of correct cell type composition in mucociliary epithelia, we were interested to elucidate if prolonged exposure to elevated Wnt signaling would alter BC behavior rendering them incompetent to (re-) generate a normal mucociliary epithelium. To address that, we treated *Xenopus* embryos with BIO starting at st. 8 but removed the drug from the medium at various stages and assessed cell type composition by immunofluorescence and ISH. Treatment with BIO from st. 8 until st. 30 caused reduced MCC, Ionocyte, and SSC numbers, which recovered after wash-out of the drug

Figure 5. Knockdown of *ΔN-tp63* Stimulates MCC and Ionocyte Specification at the Expense of BC and SSCs in *Xenopus*

(A–D) Analysis of cell type composition by confocal microscopy and staining for MCCs (Ac.-α-tubulin, green), Ionocytes (no staining, black), SSCs (large vesicles, PNA staining, magenta), and Goblet (outer-layer) cells (small granules, PNA staining, magenta) at st. 34 (A) and st. 30 (B). Actin staining (green).

(A) *ΔN-tp63* MO increases MCC and Ionocyte numbers but reduces numbers of SSCs.

(B) BIO application from st. 11 does not affect MCC and Ionocyte numbers but prevents specification of SSCs.

(C and D) Quantification from (A) and (B), respectively. Mann Whitney test, not significant, ns ($p > 0.05$); *$p \leq 0.05$; **$p \leq 0.01$; ***$p \leq 0.001$.

(E) RNA sequencing at st. 10, 17, and 25 on *Xenopus* mucociliary organoids comparing controls to *ΔN-tp63* MO injected. n = 3 per stage and treatment. Heatmap and hierarchical clustering of log2 fold changes (fcs) in cell type gene expression in *ΔN-tp63* morphants relative to controls. "Upregulated" clusters (red); "downregulated" cluster (blue).

Related to Figure S5.

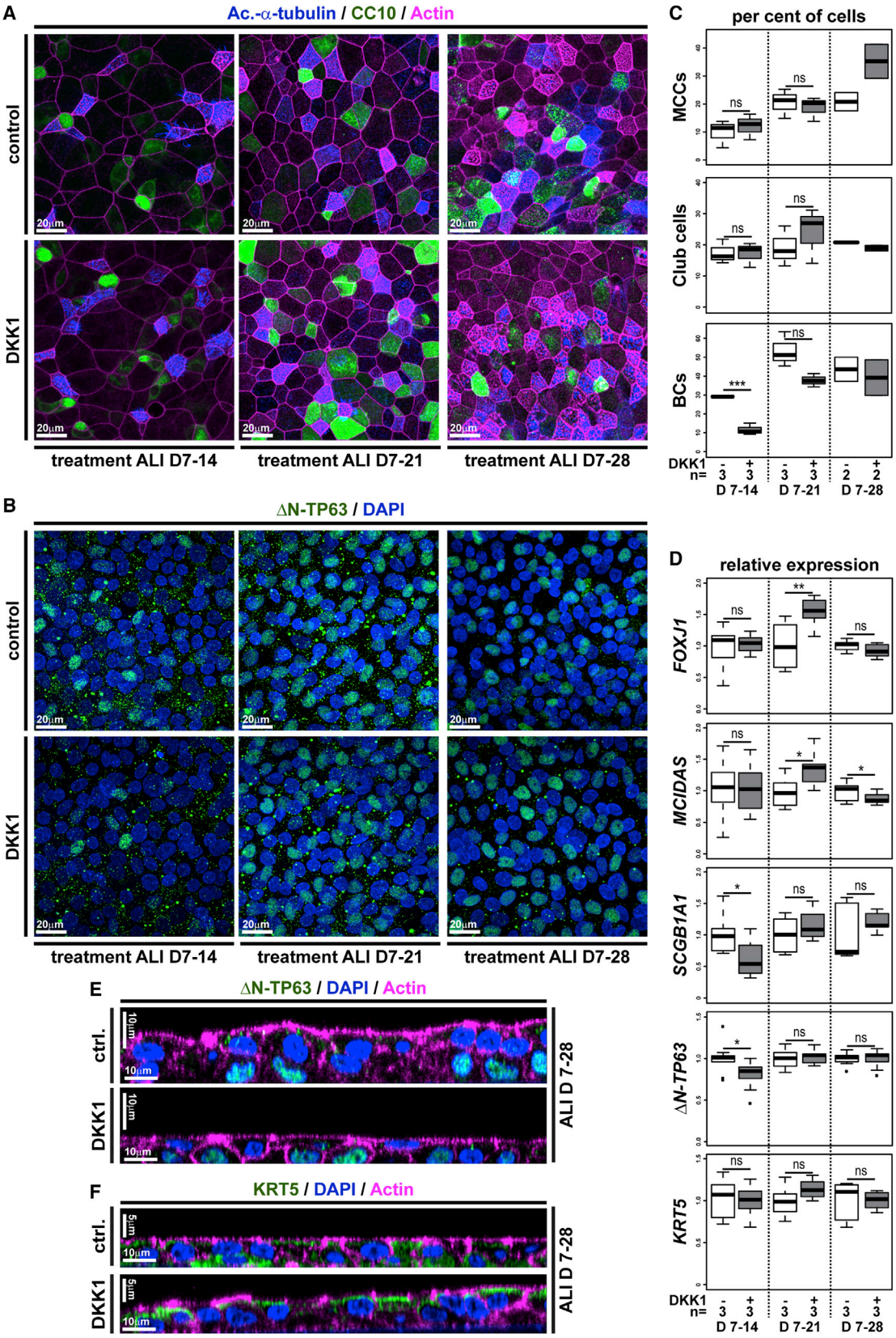

(legend on next page)

and subsequent regeneration until st. 33 (Figure 7A; Figure S6A). Similarly, treatment with BIO from st. 8 until st. 17 confirmed reduced expression of cell type specification markers as well as a thickening of the *ΔN-tp63* expressing sensorial layer. Removal of the drug at st. 17 and regeneration until st. 25 brought back the expression of epithelial cell type markers and reduced sensorial layer thickness and *ΔN-tp63* expression close to normal levels (Figure 7B; Figures S6B–S6D). To test if this remarkable regenerative ability was limited to *Xenopus* development, we conducted analogous experiments in BCI ALI cultures. BCI cultures were treated with RSPO2 from ALI day 7 until day 21, resulting in deficient formation of MCCs and Club cells. Then, RSPO2 was removed from the medium and BCIs were allowed to recover for 7 days. After removal of RSPO2, BCIs were able to successfully regenerate MCCs and Club cells and to express cell type markers for epithelial cell types, without drastic changes in proliferation or epithelial cell numbers (Figure 7C; Figures S7A–S7F). Additionally, orthogonal optical sections of RSPO2-treated BCIs after recovery revealed a normalization of epithelial thickness and KRT5 staining (Figures 7D and 7E). Collectively, our work revealed that excessive levels of Wnt signaling cause overactivation of ΔN-TP63 and block specification of epithelial cell types in a reversible manner, without altering the potential of BCs to form MCCs and secretory cells.

DISCUSSION

Our work demonstrates a requirement for dynamically regulated Wnt/β-catenin signaling in MCCs and BCs cells of the developing and regenerating mucociliary epithelium as well as a pro-proliferative effect of Wnt/β-catenin in mucociliary epithelia. Elevated Wnt/β-catenin signaling blocks cell fate specification of ciliated and secretory cells from BCs, while Wnt signaling during stages of differentiation promotes MCCs differentiation and ciliogenesis.

In BCs, high Wnt/β-catenin levels promote the expression of *ΔN-tp63*, a hallmark marker for BCs in various epithelia, including the mammalian respiratory tract (Hogan et al., 2014; Soares and Zhou, 2018; Zuo et al., 2015). We also provide evidence that *ΔN-tp63* is necessary and sufficient to promote BC fate and to inhibit specification into mature epithelial cells, including MCCs and secretory cells. *ΔN-tp63* was previously shown to be directly regulated by β-catenin in ChIP-seq studies in mammals and *Xenopus* and by promoter analysis (Kjolby and Harland, 2017; Ruptier et al., 2011). ΔN-tp63 is also known to inhibit differentiation and to promote proliferation in various cancers as well as in skin BCs (keratinocytes); in part this is regulated by transcription of cell cycle and pro-proliferative genes, which are also regulated by ΔN-tp63 in *Xenopus* (Chen et al., 2018; Soares and Zhou, 2018). To clarify whether these inhibitory effects are primarily caused by promoting proliferation or direct suppression of differentiation genes by ΔN-tp63 has to be further investigated in the future. Nevertheless, our work provides a mechanistic explanation for the negative effects of elevated Wnt/β-catenin on mucociliary differentiation reported in multiple studies and implicates ΔN-tp63 as potential driver of proliferation after mucociliary injury. Interestingly, ΔN-tp63 is not required for initial formation of a mucociliary epithelium during development (Daniely et al., 2004). Nevertheless, we found that ΔN-tp63 expression is required for maintenance of BCs and that a loss of ΔN-tp63 leads to excessive cell fate specification and differentiation of MCCs and Ionocytes causing a deficiency in late-specified SSCs in the *Xenopus* epidermis, thereby altering mucociliary cell type composition. Similar observations were made in developing *tp63*$^{-/-}$ mice, in which airway mucociliary epithelia formed during development, but those epithelia presented an excess of MCCs and a loss of BCs (Daniely et al., 2004). Furthermore, knockdown of *TP63* in ALI cultures of human airway cells prevents regeneration and causes senescence, indicating loss of stemness (Arason et al., 2014). Collectively, these findings support the conclusion that ΔN-tp63 is a Wnt/β-catenin-regulated master transcription factor in BCs, deciding between BC maintenance and differentiation. Interestingly, Wnt/β-catenin is dispensable to maintain *ΔN-TP63* and BCs after epithelialization in regenerating BCIs, suggesting that *ΔN-TP63* can be maintained by other pathways when BCs are confluent. This could be achieved by Notch signaling, which was previously shown to regulate BCs (Rock et al., 2011) but requires cell-cell contact provided by a sufficient density of cells. Furthermore, our data demonstrate a deep evolutionary conservation of signaling and regulatory mechanisms across vertebrate mucociliary epithelia, establish the *Xenopus* epidermis as a model to study BCs *in vivo*, and provide a set of conserved BC genes, which can be used as BC markers in *Xenopus* and studied mechanistically in the future.

In MCCs, Wnt/β-catenin signaling during differentiation stages is required for normal ciliation. These results are in line with previous work demonstrating that Wnt/β-catenin signaling is necessary for normal ciliogenesis in various vertebrate systems by co-regulating *foxj1*, a master transcription factor for motile cilia (Caron et al., 2012; Sun et al., 2018; Walentek et al., 2015). The positive effect of Wnt/β-catenin on

Figure 6. Inhibition of Wnt/β-Catenin Signaling Transiently Reduces Stemness and Promotes Differentiation in Human BCs

(A–F) BCIs in ALI culture for up to 4 weeks. Human recombinant DKK1 (DKK1) was used to inhibit Wnt/β-catenin signaling starting at ALI day 7 (D7).

(A) Confocal imaging of specimens stained for Ac.-α-tubulin (MCCs, blue), CC10 (Club cells, green), and Actin (cell membranes, magenta) shows moderately increased MCC and Club cell numbers after DKK1 treatment.

(B) DKK1 leads to a transient decrease in BCs but does not lead to loss of ΔN-TP63+ (green) cells. Nuclei (DAPI, blue).

(C) Quantification from (A) and (B), respectively. Mann Whitney test, not significant, ns ($p > 0.05$); ***$p \leq 0.001$.

(D) Quantitative real-time PCR expression levels are depicted relative to stage controls. DKK1 increases expression of MCC (*FOXJ1*, *MCIDAS*) and to a lesser extent Club cell (*SCGB1A1*) markers but without reduction of BC markers (*ΔN-TP63*, *KRT5*). Student's t test, not significant, ns ($p > 0.05$); *$p \leq 0.05$; **$p \leq 0.01$.

(E and F) Optical orthogonal sections of confocal images after staining for BC markers ΔN-TP63 (green, in E) and KRT5 (green, in F).

Related to Figure S5.

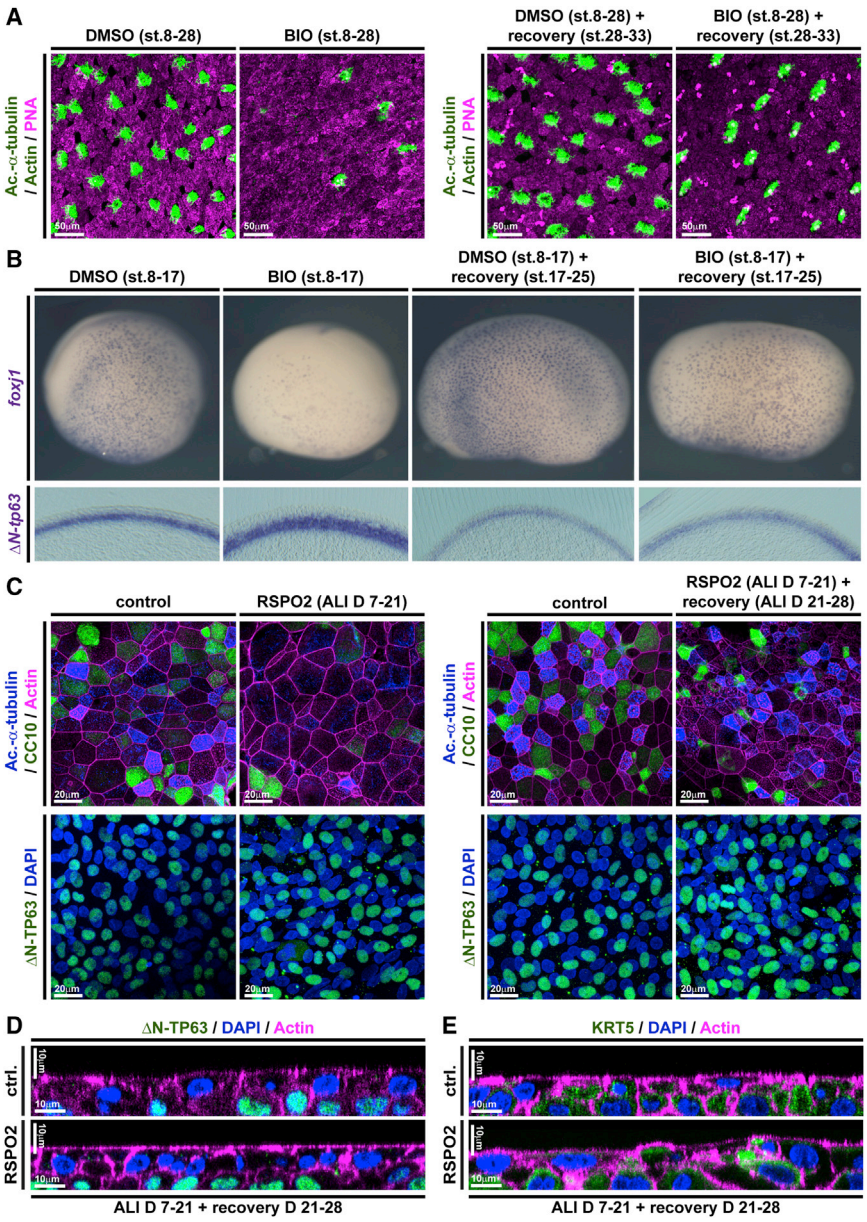

Figure 7. Wnt/β-Catenin-Induced Increase in BCs and Loss of Epithelial Differentiation Are Reversible

(A and B) In *Xenopus*, BIO treatments from st. 8–17 or st. 8–30 inhibit differentiation as compared to DMSO treated controls, but the epithelium can regenerate after removal of BIO and recovery until st. 33 (A) or st. 25 (B).

(A) BIO treatment reduces MCC (Ac.-α-tubulin, green), Ionocyte (no staining, black), and SSC (large vesicles, PNA staining, magenta) numbers in confocal micrographs at st. 28, which recover after regeneration until st. 33. Actin staining (green).

(B) ISH shows reduction in *foxj1* expressing cells and an increase in *ΔN-tp63* expression in BIO-treated whole mounts (upper row) and transversal sections (bottom row) at st. 17, which both recover after regeneration until st. 25. DMSO (n = 5); BIO st. 17 (n = 5); DMSO st. 25 (n = 5); BIO+recovery st. 25 (n = 5).

(C) Confocal imaging of specimens stained for Ac.-α-tubulin (MCCs, blue), CC10 (Club cells, green), and Actin (cell membranes, magenta) show reduced MCC and Club cell numbers in RSPO2-treated cultures from ALI D7 to D21 but regeneration of MCCs and Club cells at ALI D28. n = 3 cultures per time point and treatment (upper panels). No loss of ΔN-TP63+ (green) BCs is observed in these experiments (bottom panels). Nuclei (DAPI, blue).

(D and E) Optical orthogonal sections of confocal images. RSPO2-treated cultures display normalized epithelial thickness and staining for BC markers ΔN-TP63 (green, in D) and KRT5 (green, in E) after regeneration at ALI D28.

Related to Figures S6 and S7.

MCC specification suggested by some studies could be explained by the extensive positive cross-regulation between transcription factors expressed in MCCs. The multiciliogenesis cascade is initiated by a transcriptional regulatory complex consisting of Multicilin (encoded by *mcidas*), E2f4/5, and TfDp1, which activates expression of the downstream transcription factors *foxj1*, *rfx2/3*, *myb*, *tp73*, and *foxn4* (Quigley and Kintner, 2017; Stubbs et al., 2012; Walentek and Quigley, 2017). These transcription factors generate a positive feedback on their expression (Choksi et al., 2014; Quigley and Kintner, 2017). This positive cross-regulation was especially well demonstrated for FOXJ1 and RFX2/3 and argues for the possibility that activation of *FOXJ1* could ultimately lead to activation of the multiciliogenesis cascade (Didon et al., 2013).

Additionally, we have previously found that *myb* expression is downregulated after inhibition of Wnt/β-catenin signaling, suggesting that *myb* could be regulated by Wnt signaling as well (Tan et al., 2013; Walentek et al., 2015). Thus, different levels and timing of Wnt/β-catenin signaling activation could provide an explanation as to why some studies reported negative effects on MCC formation, while others described an increase in MCC numbers.

Our data argue that the loss of differentiated MCCs upon excessive Wnt activation is a consequence of impaired specification, rather than Goblet cell hyperplasia as previously suggested (Mucenski et al., 2005). While we did not observe an increase in MUC5B expressing cells in the epithelium after Wnt activation, we did detect elevated *MUC5B* expression levels. This suggests potential induction of subepithelial Goblet cell formation *in vitro* after overactivation of Wnt/β-catenin signaling, similar to the induction of Goblet cells in submucosal glands (Driskell et al., 2004).

Finally, our data indicate that persistent Wnt/β-catenin activation in mucociliary epithelia could lead to BC hyperplasia and

a remodeling of the epithelium. Importantly, we show that these effects are reversible and that a return to normal signaling levels can promote re-establishment of a differentiated epithelium. This is an important notion in the context of chronic lung diseases, such as COPD and IPF. IPF leads to a destruction of lung tissue starting at the alveoli, which is strongly associated with upregulated Wnt signaling, extracellular matrix deposition, and failure of alveolar stem cells to regenerate correctly, while COPD is associated with defective mucociliary epithelial differentiation, BC hyperplasia, altered Wnt ligand expression, and overactivation of the Wnt/β-catenin pathway (Baarsma and Königshoff, 2017; Chen et al., 2010; Heijink et al., 2013; Königshoff et al., 2008). Furthermore, it was shown that nasal polyps from chronic rhinosinusitis patients produce excess levels of WNT3a and MCC differentiation is inhibited but that MCC formation could be rescued by application of a Wnt inhibitor (Dobzanski et al., 2018). Together, these findings suggest that even in a chronically pathogenic state, targeted Wnt/β-catenin signaling inhibition could provide a potential avenue for treatment of patients with COPD and other chronic lung diseases for which treatment options are currently limited or absent.

STAR★METHODS

Detailed methods are provided in the online version of this paper and include the following:

- KEY RESOURCES TABLE
- LEAD CONTACT AND MATERIALS AVAILABILITY
- EXPERIMENTAL MODELS AND SUBJECT DETAILS
  - Xenopus laevis
  - Mice
  - Immortalized Human Basal Cells (BCIs)
  - Ethics Statements on Animal Experiments
- METHOD DETAILS
  - Manipulation of *Xenopus* Embryos, Constructs, and In Situ Hybridization
  - Generation of the Xenopus Wnt/β-catenin Signaling Reporter Line
  - RNA-Sequencing on Xenopus Mucociliary Organoids and Bioinformatics Analysis
  - Air-Liquid Interface (ALI) Culture of Immortalized Human Basal Cells (BCIs)
  - ALI Culture of Primary Mouse Tracheal Epithelial Cells (MTECs)
  - Quantitative RT-PCR on cDNAs from BCIs
  - Immunofluorescence Staining and Sample Preparation
  - Confocal Imaging, Image Processing, and Analysis
- QUANTIFICATION AND STATISTICAL ANALYSIS
  - Statistical Evaluation
  - Sample Size and Analysis
  - Use of Shared Controls
- DATA AND SOFTWARE AVAILABILITY

SUPPLEMENTAL INFORMATION

Supplemental Information can be found online at https://doi.org/10.1016/j.celrep.2019.08.063.

ACKNOWLEDGMENTS

We thank S. Schefold, D. and E. Pangilinan, and J. Groth for technical help; R. Kjolby, W. Finkbeiner, C. Boecking, G. Pyrowolakis, L. Kodjabachian, R. Harland, S. Arnolds, and B. Gomperts for discussions and sharing of unpublished results; R. Crystal and M. Walters for BCi-NS1.1 cells; T. Kwon and S. Medina Ruiz for genome annotation files; NXR (RRID: SCR_013731), Xenbase (RRID: SCR_004337), and EXRC for *Xenopus* resources; Transcriptome and Genome Analysis laboratory Göttingen for deep sequencing; Light Imaging Center Freiburg for microscope use; JAX (RRID: SCR_004633) for mice; and Galaxy Europe for the bioinformatics platform. This study was supported by the German Research Foundation (DFG) under the Emmy Noether Programme (grant WA3365/2-1) and under Germany's Excellence Strategy (CIBSS – EXC-2189 – Project ID 390939984), as well as by an NHLBI Pathway to Independence Award (K99HL127275) to P.W. Generation of transgenic *Xenopus* was supported by FWO-Vlaanderen grant G029413N and by the Concerted Research Actions from Ghent University (BOF15/GOA/011) to K.V. D.I.S. was supported by the URAP program and a Pergo Foundation SURF L&S Fellowship. The article processing charge was funded by the German Research Foundation (DFG) and the University of Freiburg in the funding programme Open Access Publishing.

AUTHOR CONTRIBUTIONS

M.H., D.I.S., M.B., A.T., and P.W. performed *Xenopus* experiments. J.L.G.V., A.T., and P.W. performed tissue culture experiments. J.L.G.V. and P.W. performed the mouse Wnt reporter analysis. H.T.T. and K.V. generated the *Xenopus laevis* Wnt reporter line. O.S. and P.W. provided bioinformatics. M.H. and P.W. performed experimental design and planning. P.W. provided study design and supervision, coordinated collaborative work, and prepared the manuscript.

DECLARATION OF INTERESTS

The authors declare no competing interests.

Received: June 4, 2019
Revised: August 4, 2019
Accepted: August 21, 2019
Published: September 24, 2019

REFERENCES

Andrews, S. (2010). FastQC: a quality control tool for high throughput sequence data, Available at. http://www.bioinformatics.babraham.ac.uk/projects/fastqc.

Antoniades, I., Stylianou, P., and Skourides, P.A. (2014). Making the connection: ciliary adhesion complexes anchor basal bodies to the actin cytoskeleton. Dev. Cell *28*, 70–80.

Arason, A.J., Jonsdottir, H.R., Halldorsson, S., Benediktsdottir, B.E., Bergthorsson, J.T., Ingthorsson, S., Baldursson, O., Sinha, S., Gudjonsson, T., and Magnusson, M.K. (2014). deltaNp63 has a role in maintaining epithelial integrity in airway epithelium. PLoS ONE *9*, e88683.

Baarsma, H.A., and Königshoff, M. (2017). *'WNT-er is coming'*: WNT signalling in chronic lung diseases. Thorax *72*, 746–759.

Borday, C., Parain, K., Thi Tran, H., Vleminckx, K., Perron, M., and Monsoro-Burq, A.H. (2018). An atlas of Wnt activity during embryogenesis in Xenopus tropicalis. PLoS ONE *13*, e0193606.

Brechbuhl, H.M., Ghosh, M., Smith, M.K., Smith, R.W., Li, B., Hicks, D.A., Cole, B.B., Reynolds, P.R., and Reynolds, S.D. (2011). β-catenin dosage is a critical determinant of tracheal basal cell fate determination. Am. J. Pathol. *179*, 367–379.

Caron, A., Xu, X., and Lin, X. (2012). Wnt/β-catenin signaling directly regulates Foxj1 expression and ciliogenesis in zebrafish Kupffer's vesicle. Development *139*, 514–524.

Chen, Y.T., Gallup, M., Nikulina, K., Lazarev, S., Zlock, L., Finkbeiner, W., and McNamara, N. (2010). Cigarette smoke induces epidermal growth factor receptor-dependent redistribution of apical MUC1 and junctional β-catenin in polarized human airway epithelial cells. Am. J. Pathol. *177*, 1255–1264.

Chen, Y., Peng, Y., Fan, S., Li, Y., Xiao, Z.X., and Li, C. (2018). A double dealing tale of p63: an oncogene or a tumor suppressor. Cell. Mol. Life Sci. *75*, 965–973.

Choksi, S.P., Lauter, G., Swoboda, P., and Roy, S. (2014). Switching on cilia: transcriptional networks regulating ciliogenesis. Development *141*, 1427–1441.

Cibois, M., Luxardi, G., Chevalier, B., Thomé, V., Mercey, O., Zaragosi, L.-E., Barbry, P., Pasini, A., Marcet, B., and Kodjabachian, L. (2015). BMP signalling controls the construction of vertebrate mucociliary epithelia. Development *142*, 2352–2363.

Clevers, H. (2006). Wnt/β-catenin signaling in development and disease. Cell *127*, 469–480.

Daniely, Y., Liao, G., Dixon, D., Linnoila, R.I., Lori, A., Randell, S.H., Oren, M., and Jetten, A.M. (2004). Critical role of p63 in the development of a normal esophageal and tracheobronchial epithelium. Am. J. Physiol. Cell Physiol. *287*, C171–C181.

Deblandre, G.A., Wettstein, D.A., Koyano-Nakagawa, N., and Kintner, C. (1999). A two-step mechanism generates the spacing pattern of the ciliated cells in the skin of Xenopus embryos. Development *126*, 4715–4728.

Didon, L., Zwick, R.K., Chao, I.W., Walters, M.S., Wang, R., Hackett, N.R., and Crystal, R.G. (2013). RFX3 modulation of FOXJ1 regulation of cilia genes in the human airway epithelium. Respir. Res. *14*, 70.

Dobin, A., Davis, C.A., Schlesinger, F., Drenkow, J., Zaleski, C., Jha, S., Batut, P., Chaisson, M., and Gingeras, T.R. (2013). STAR: ultrafast universal RNA-seq aligner. Bioinformatics *29*, 15–21.

Dobzanski, A., Khalil, S.M., and Lane, A.P. (2018). Nasal polyp fibroblasts modulate epithelial characteristics via Wnt signaling. Int. Forum Allergy Rhinol. *8*, 1412–1420.

Driskell, R.R., Liu, X., Luo, M., Filali, M., Zhou, W., Abbott, D., Cheng, N., Moothart, C., Sigmund, C.D., and Engelhardt, J.F. (2004). Wnt-responsive element controls Lef-1 promoter expression during submucosal gland morphogenesis. Am. J. Physiol. Lung Cell. Mol. Physiol. *287*, L752–L763.

Dubaissi, E., Rousseau, K., Lea, R., Soto, X., Nardeosingh, S., Schweickert, A., Amaya, E., Thornton, D.J., and Papalopulu, N. (2014). A secretory cell type develops alongside multiciliated cells, ionocytes and goblet cells, and provides a protective, anti-infective function in the frog embryonic mucociliary epidermis. Development *141*, 1514–1525.

Ferrer-Vaquer, A., Piliszek, A., Tian, G., Aho, R.J., Dufort, D., and Hadjantonakis, A.K. (2010). A sensitive and bright single-cell resolution live imaging reporter of Wnt/ß-catenin signaling in the mouse. BMC Dev. Biol. *10*, 121.

Gomperts, B.N., Gong-Cooper, X., and Hackett, B.P. (2004). Foxj1 regulates basal body anchoring to the cytoskeleton of ciliated pulmonary epithelial cells. J. Cell Sci. *117*, 1329–1337.

Hackett, N.R., Shaykhiev, R., Walters, M.S., Wang, R., Zwick, R.K., Ferris, B., Witover, B., Salit, J., and Crystal, R.G. (2011). The human airway epithelial basal cell transcriptome. PLoS ONE *6*, e18378.

Harland, R.M. (1991). In situ hybridization: an improved whole-mount method for Xenopus embryos. Methods Cell Biol. *36*, 685–695.

Hashimoto, S., Chen, H., Que, J., Brockway, B.L., Drake, J.A., Snyder, J.C., Randell, S.H., and Stripp, B.R. (2012). β-Catenin-SOX2 signaling regulates the fate of developing airway epithelium. J. Cell Sci. *125*, 932–942.

Hayes, J.M., Kim, S.K., Abitua, P.B., Park, T.J., Herrington, E.R., Kitayama, A., Grow, M.W., Ueno, N., and Wallingford, J.B. (2007). Identification of novel ciliogenesis factors using a new in vivo model for mucociliary epithelial development. Dev. Biol. *312*, 115–130.

Heasman, J., Kofron, M., and Wylie, C. (2000). β-catenin signaling activity dissected in the early Xenopus embryo: a novel antisense approach. Dev. Biol. *222*, 124–134.

Heijink, I.H., de Bruin, H.G., van den Berge, M., Bennink, L.J.C., Brandenburg, S.M., Gosens, R., van Oosterhout, A.J., and Postma, D.S. (2013). Role of aberrant WNT signalling in the airway epithelial response to cigarette smoke in chronic obstructive pulmonary disease. Thorax *68*, 709–716.

Hirsch, N., Zimmerman, L.B., and Grainger, R.M. (2002). Xenopus, the next generation: X. tropicalis genetics and genomics. Dev. Dyn. *225*, 422–433.

Hogan, B.L.M., Barkauskas, C.E., Chapman, H.A., Epstein, J.A., Jain, R., Hsia, C.C.W., Niklason, L., Calle, E., Le, A., Randell, S.H., et al. (2014). Repair and regeneration of the respiratory system: complexity, plasticity, and mechanisms of lung stem cell function. Cell Stem Cell *15*, 123–138.

Hong, K.U., Reynolds, S.D., Watkins, S., Fuchs, E., and Stripp, B.R. (2004). Basal cells are a multipotent progenitor capable of renewing the bronchial epithelium. Am. J. Pathol. *164*, 577–588.

Hou, Z., Wu, Q., Sun, X., Chen, H., Li, Y., Zhang, Y., Mori, M., Yang, Y., Que, J., and Jiang, M. (2019). Wnt/Fgf crosstalk is required for the specification of basal cells in the mouse trachea. Development *146*, dev171496.

Huang, Y.L., and Niehrs, C. (2014). Polarized Wnt signaling regulates ectodermal cell fate in Xenopus. Dev. Cell *29*, 250–257.

Kjolby, R.A.S., and Harland, R.M. (2017). Genome-wide identification of Wnt/β-catenin transcriptional targets during Xenopus gastrulation. Dev. Biol. *426*, 165–175.

Kolm, P.J., and Sive, H.L. (1995). Efficient hormone-inducible protein function in Xenopus laevis. Dev. Biol. *171*, 267–272.

Königshoff, M., Balsara, N., Pfaff, E.M., Kramer, M., Chrobak, I., Seeger, W., and Eickelberg, O. (2008). Functional Wnt signaling is increased in idiopathic pulmonary fibrosis. PLoS ONE *3*, e2142.

Liao, Y., Smyth, G.K., and Shi, W. (2014). featureCounts: an efficient general purpose program for assigning sequence reads to genomic features. Bioinformatics *30*, 923–930.

Love, M.I., Huber, W., and Anders, S. (2014). Moderated estimation of fold change and dispersion for RNA-seq data with DESeq2. Genome Biol. *15*, 550.

Lu, P., Barad, M., and Vize, P.D. (2001). Xenopus p63 expression in early ectoderm and neurectoderm. Mech. Dev. *102*, 275–278.

Lynch, T.J., Anderson, P.J., Rotti, P.G., Tyler, S.R., Crooke, A.K., Choi, S.H., Montoro, D.T., Silverman, C.L., Shahin, W., Zhao, R., et al. (2018). Submucosal Gland Myoepithelial Cells Are Reserve Stem Cells That Can Regenerate Mouse Tracheal Epithelium. Cell Stem Cell *22*, 653–667.e5.

Mall, M.A. (2008). Role of cilia, mucus, and airway surface liquid in mucociliary dysfunction: lessons from mouse models. J. Aerosol Med. Pulm. Drug Deliv. *21*, 13–24.

Malleske, D.T., Hayes, D., Jr., Lallier, S.W., Hill, C.L., and Reynolds, S.D. (2018). Regulation of Human Airway Epithelial Tissue Stem Cell Differentiation by β-Catenin, P300, and CBP. Stem Cells *36*, 1905–1916.

Mi, H., Muruganujan, A., Casagrande, J.T., and Thomas, P.D. (2013). Large-scale gene function analysis with the PANTHER classification system. Nat. Protoc. *8*, 1551–1566.

Mucenski, M.L., Nation, J.M., Thitoff, A.R., Besnard, V., Xu, Y., Wert, S.E., Harada, N., Taketo, M.M., Stahlman, M.T., and Whitsett, J.A. (2005). β-catenin regulates differentiation of respiratory epithelial cells in vivo. Am. J. Physiol. Lung Cell. Mol. Physiol. *289*, L971–L979.

Niehrs, C. (2012). The complex world of WNT receptor signalling. Nat. Rev. Mol. Cell Biol. *13*, 767–779.

Pongracz, J.E., and Stockley, R.A. (2006). Wnt signalling in lung development and diseases. Respir. Res. *7*, 15.

Quigley, I.K., and Kintner, C. (2017). Rfx2 Stabilizes Foxj1 Binding at Chromatin Loops to Enable Multiciliated Cell Gene Expression. PLoS Genet. *13*, e1006538.

Quigley, I.K., Stubbs, J.L., and Kintner, C. (2011). Specification of ion transport cells in the Xenopus larval skin. Development *138*, 705–714.

Reynolds, S.D., Zemke, A.C., Giangreco, A., Brockway, B.L., Teisanu, R.M., Drake, J.A., Mariani, T., Di, P.Y.P., Taketo, M.M., and Stripp, B.R. (2008).

Conditional stabilization of β-catenin expands the pool of lung stem cells. Stem Cells *26*, 1337–1346.

Rock, J.R., Onaitis, M.W., Rawlins, E.L., Lu, Y., Clark, C.P., Xue, Y., Randell, S.H., and Hogan, B.L.M. (2009). Basal cells as stem cells of the mouse trachea and human airway epithelium. Proc. Natl. Acad. Sci. USA *106*, 12771–12775.

Rock, J.R., Randell, S.H., and Hogan, B.L.M. (2010). Airway basal stem cells: a perspective on their roles in epithelial homeostasis and remodeling. Dis. Model. Mech. *3*, 545–556.

Rock, J.R., Gao, X., Xue, Y., Randell, S.H., Kong, Y.Y., and Hogan, B.L.M. (2011). Notch-dependent differentiation of adult airway basal stem cells. Cell Stem Cell *8*, 639–648.

Ruptier, C., De Gaspéris, A., Ansieau, S., Granjon, A., Tanière, P., Lafosse, I., Shi, H., Petitjean, A., Taranchon-Clermont, E., Tribollet, V., et al. (2011). TP63 P2 promoter functional analysis identifies β-catenin as a key regulator of ΔNp63 expression. Oncogene *30*, 4656–4665.

Schmid, A., Sailland, J., Novak, L., Baumlin, N., Fregien, N., and Salathe, M. (2017). Modulation of Wnt signaling is essential for the differentiation of ciliated epithelial cells in human airways. FEBS Lett. *591*, 3493–3506.

Sive, H.L., Grainger, R.M., and Harland, R.M. (2010). Microinjection of xenopus oocytes. Cold Spring Harb. Protoc. *2010*, pdb.ip8.

Soares, E., and Zhou, H. (2018). Master regulatory role of p63 in epidermal development and disease. Cell. Mol. Life Sci. *75*, 1179–1190.

Stubbs, J.L., Davidson, L., Keller, R., and Kintner, C. (2006). Radial intercalation of ciliated cells during Xenopus skin development. Development *133*, 2507–2515.

Stubbs, J.L., Oishi, I., Izpisúa Belmonte, J.C., and Kintner, C. (2008). The forkhead protein Foxj1 specifies node-like cilia in Xenopus and zebrafish embryos. Nat. Genet. *40*, 1454–1460.

Stubbs, J.L., Vladar, E.K., Axelrod, J.D., and Kintner, C. (2012). Multicilin promotes centriole assembly and ciliogenesis during multiciliate cell differentiation. Nat. Cell Biol. *14*, 140–147.

Sun, D.I., Tasca, A., Haas, M., Baltazar, G., Harland, R.M., Finkbeiner, W.E., and Walentek, P. (2018). Na+/H+ Exchangers Are Required for the Development and Function of Vertebrate Mucociliary Epithelia. Cells Tissues Organs *205*, 279–292.

Tan, F.E., Vladar, E.K., Ma, L., Fuentealba, L.C., Hoh, R., Espinoza, F.H., Axelrod, J.D., Alvarez-Buylla, A., Stearns, T., Kintner, C., and Krasnow, M.A. (2013). Myb promotes centriole amplification and later steps of the multiciliogenesis program. Development *140*, 4277–4286.

Tilley, A.E., Walters, M.S., Shaykhiev, R., and Crystal, R.G. (2015). Cilia dysfunction in lung disease. Annu. Rev. Physiol. *77*, 379–406.

Tran, H.T., Sekkali, B., Van Imschoot, G., Janssens, S., and Vleminckx, K. (2010). Wnt/beta-catenin signaling is involved in the induction and maintenance of primitive hematopoiesis in the vertebrate embryo. Proc. Natl. Acad. Sci. USA *107*, 16160–16165.

Vladar, E.K., and Brody, S.L. (2013). Analysis of Ciliogenesis in Primary Culture Mouse Tracheal Epithelial Cells (Elsevier Inc.).

Walentek, P. (2018). Manipulating and Analyzing Cell Type Composition of the Xenopus Mucociliary Epidermis. In Xenopus: Methods and Protocols, K. Vleminckx, ed. (Methods in Molecular Biology), pp. 251–263.

Walentek, P., and Quigley, I.K. (2017). What we can learn from a tadpole about ciliopathies and airway diseases: Using systems biology in Xenopus to study cilia and mucociliary epithelia. Genesis *55*, 1–13.

Walentek, P., Beyer, T., Thumberger, T., Schweickert, A., and Blum, M. (2012). ATP4a is required for Wnt-dependent Foxj1 expression and leftward flow in Xenopus left-right development. Cell Rep. *1*, 516–527.

Walentek, P., Bogusch, S., Thumberger, T., Vick, P., Dubaissi, E., Beyer, T., Blum, M., and Schweickert, A. (2014). A novel serotonin-secreting cell type regulates ciliary motility in the mucociliary epidermis of Xenopus tadpoles. Development *141*, 1526–1533.

Walentek, P., Beyer, T., Hagenlocher, C., Müller, C., Feistel, K., Schweickert, A., Harland, R.M., and Blum, M. (2015). ATP4a is required for development and function of the Xenopus mucociliary epidermis - a potential model to study proton pump inhibitor-associated pneumonia. Dev. Biol. *408*, 292–304.

Walters, M.S., Gomi, K., Ashbridge, B., Moore, M.A.S., Arbelaez, V., Heldrich, J., Ding, B.S., Rafii, S., Staudt, M.R., and Crystal, R.G. (2013). Generation of a human airway epithelium derived basal cell line with multipotent differentiation capacity. Respir. Res. *14*, 135.

Warburton, D., El-Hashash, A., Carraro, G., Tiozzo, C., Sala, F., Rogers, O., De Langhe, S., Kemp, P.J., Riccardi, D., Torday, J., et al. (2010). Lung Organogenesis. Curr. Top. Dev. Biol. *90*, 73–158.

Warner, S.M.B., Hackett, T.L., Shaheen, F., Hallstrand, T.S., Kicic, A., Stick, S.M., and Knight, D.A. (2013). Transcription factor p63 regulates key genes and wound repair in human airway epithelial basal cells. Am. J. Respir. Cell Mol. Biol. *49*, 978–988.

Zuo, W., Zhang, T., Wu, D.Z.A., Guan, S.P., Liew, A.A., Yamamoto, Y., Wang, X., Lim, S.J., Vincent, M., Lessard, M., et al. (2015). p63(+)Krt5(+) distal airway stem cells are essential for lung regeneration. Nature *517*, 616–620.

STAR★METHODS

KEY RESOURCES TABLE

REAGENT or RESOURCE	SOURCE	IDENTIFIER
Antibodies		
mouse anti-Acetylated-α-tubulin (1:700 – 1:1000, XL, HS, MM)	Sigma/Merck	T6793
rabbit anti-GFP (1:500, XL)	Abcam	ab290
rabbit anti-Cytokeratin 5 (1:500, HS)	Thermo Fisher	PA1-37974
rabbit anti-human Club Cell Protein (1:1000, HS)	BioVendor	RD181022220-01
rabbit anti-human p63 (pan-p63, 1:500, HS)	Proteintech	12143-1-AP
rabbit anti-mouse Uteroglobin (1:500, MM)	Abcam	ab40873
mouse anti-Ki-67 (1:1000, HS)	Cell Signaling	9449
mouse anti-Muc5B (1:500, HS)	Santa Cruz Biotech	sc-393952
rabbit anti-Serotonin (1:500, XL)	Merk/Milipore	AB938
AlexaFluor 555-labeled goat anti-mouse	Molecular Probes	A21422
AlexaFluor 488-labeled donkey anti-mouse	Molecular Probes	R37114
AlexaFluor 488-labeled goat anti-rabbit	Molecular Probes	R37116
AlexaFluor 405-labeled goat anti-mouse	Molecular Probes	A31553
Bacterial Strains		
NEB® 5-alpha Competent *E. coli* (High Efficiency)	New England Biolabs	C2987H
Chemicals, Peptides, and Recombinant Proteins		
6-Bromoindirubin-3′-oxime (BIO)	Sigma-Aldrich/Merck	B1686
Dexamethasone	Sigma-Aldrich/Merck	D4902
RNase Inhibitor	Promega	N251B
Dig-labeled rNTPs	Roche	3359247910, 11277057001
human recombinant RSPO2	R&D systems	3266-RS
human recombinant DKK1	R&D systems	5439-DK
AlexaFluor 488-labeled Phalloidin	Molecular Probes	A12379
AlexaFluor 647-labeled Phalloidin	Molecular Probes	A22287
AlexaFluor 647-labeled PNA	Molecular Probes	L32460
Critical Commercial Assays		
PureYield Midiprep kit	Promega	A2495
Ambion mMessage Machine kit	Thermo Fisher	AM1340
T7 RNA polymerase	Promega	P2077
SP6 RNA polymerase	Promega	P108G
TruSeq RNA Library Preparation Kit v2, Set A	Illumina	RS-122-2301
RNA Analysis Kit	Advanced Analytical	DNF-471
QuantiFluordsDNA System	Promega	E2670
dsDNA 905 Reagent Kit	Advanced Analytical	DNF-905
BEGM Bullet Kit	Lonza	CC-3170
RNeasy Mini Kit	QIAGEN	74104
QIAshredder	QIAGEN	79654
iScript cDNA Synthesis Kit	Bio-Rad	1708891
Sso Advanced Universal SYBR Green Supermix	Bio-Rad	1725275
Deposited Data		
RNA-sequencing data	This paper	GEO: GSE130448
Experimental Models: Cell Lines		
Human: BCi-NS1.1	Ronal Crystal laboratory	RRID:CVCL_T029

(*Continued on next page*)

Continued

REAGENT or RESOURCE	SOURCE	IDENTIFIER
Experimental Models: Organisms/Strains		
Xenopus laevis: pbin7LEF:dGFP: Xla.Tg(WntREs:dEGFP)^{Vlemx}	National *Xenopus* Resource	NXR_0064
Wild type *Xenopus laevis*	EXRC, NXR	N/A
Mouse: TCF/LEF:H2B-GFP: TCF/Lef1-HISTH2BB/ EGFP 61Hadj/J	Jackson Laboratories	013752
Oligonucleotides		
β-catenin MO: 5′-TTTCAACCGTTTCCAAAGAAC CAGG −3′	Gene Tools	N/A
ΔN-tp63 MO: 5′-GATACAACATCTTTGCAGTG AGGTT-3′	Gene Tools	N/A
ΔN-tp63-f: AAAAAAGGATCCATGTTGTATCTGGA AAACAATG	Sigma Aldrich	N/A
ΔN-tp63-stop-r: GTCGACTCATTCACCCTCTTCCT TAATAC	Sigma Aldrich	N/A
ΔN-tp63-nonstop-r: GTCGACTTCACCCTCTTCCT TAATAC	Sigma Aldrich	N/A
gfp-f: AAAAAAGGATCCATGGTGAGCAAGGGCG AGGAGCTGTTC	Sigma Aldrich	N/A
gfp-r: AAAAAAGGATCCCTTGTACAGCTCGTCCA TGCCATGCCGAGAGTG	Sigma Aldrich	N/A
gr-lbd-f: CAACGTATTAAGGAAGAGGGTGAAGT CGACACCTCTGAAAATCCTGGTAACAAAACAA TAGTTCC	Sigma Aldrich	N/A
gr-lbd-r: TTGCGGCCGCGGCCAGATTGGCCTGT CGACtCACTTTTGATGAAACAGAAGTTTTTTGAT ATTTCC	Sigma Aldrich	N/A
Quantitative RT-PCR primers, see Table S3	Sigma Aldrich	N/A
Recombinant DNA		
pCS107-ΔN-tp63	This paper	N/A
pCS107-gfp-ΔN-tp63	This paper	N/A
pCS107-gfp-ΔN-tp63-gr	This paper	N/A
Software		
bcl2fastq v2.17.1.14	http://emea.support.illumina.com/sequencing/sequencing_software/bcl2fastq-conversion-software/downloads.html	N/A
FastQC v0.11.5	http://bioinformatics.babraham.ac.uk/projects/fastqc	
RNA STAR v2.6.0b-1	http://code.google.com/archive/p/rna-star/	N/A
featureCounts v1.6.3	https://sourceforge.net/projects/subread/files/	N/A
DEseq2 v1.22.1	http://bioconductor.org/packages/release/bioc/html/DESeq2.html	N/A
R v3.5.1	https://www.rstudio.com/	N/A
ggplot2/heatmap2 v2.2.1	https://rdocumentation.org/packages/ggplot2/versions/2.2.1	N/A
ImageJ	https://imagej.nih.gov/ij/download.html	N/A
NeuronJ v1.4.3	https://imagescience.org/meijering/software/neuronj/	N/A
ZEN (black & blue)	Zeiss	N/A
Other (MTEC Media)		
Pronase (1.5mg/ml in Pronase solution)	Roche	10165921001
Ham's F12 (Pronase solution, DNase solution)	Life Technologies	11765054

(*Continued on next page*)

Continued

REAGENT or RESOURCE	SOURCE	IDENTIFIER
DNase (0.5mg/ml in DNase solution)	Sigma	DN25
DMEM:F12 (Proliferation and Differentiation medium)	GIBCO	11330-032
Penicillin-Streptomycin (1% in Proliferation and Differentiation medium, Pronase solution)	Sigma	P4333
Amphotericin B (0.1% in Proliferation and Differentiation medium)	GIBCO	15290-018
Sodium Biscarbonate (0.3% in Proliferation and Differentiation medium)	Life Technologies	25080060
Insulin (10 μg/ml in Proliferation medium)	Sigma	1182
Epidermal Growth Factor (25 μg/ml in Proliferation medium)	BD Biosciences	354001
Apo-Transferrin (5 μg/ml in Proliferation medium)	Sigma	T1147
Cholera toxin (0.1 μg/ml in Proliferation medium)	Sigma	C8052
Bovine pituitary extract (30 μg/ml in Proliferation medium)	Sigma	SLBV9702
FBS Superior (5% in Proliferation medium)	Biochrom	S0615
Retinoic acid (50nM in Proliferation and Differentiation medium)	Sigma	R2625
NuSerum (2% in Differentiation medium)	BD Biosciences	355100

LEAD CONTACT AND MATERIALS AVAILABILITY

Further information and requests for resources and reagents should be directed to and will be fulfilled by the Lead Contact, Peter Walentek (peter.walentek@medizin.uni-freiburg.de).

Immortalized human Basal cells (BCIs) were generated and are distributed by the Crystal laboratory at Genetic Medicine/Joan and Sanford I. Weill Department of Medicine, Weill Cornell Medical School, New York, USA. Sharing of this resource is subject to an MTA.

The Wnt reporter line *Xla.Tg(WntREs:dEGFP)*^{Vlemx} was obtained from the National *Xenopus* Resource (NXR) at Marine Biological Laboratory, Woods Hole, USA, and the European *Xenopus* Resource Centre (EXRC) at University of Portsmouth, School of Biological Sciences, UK. Sharing of this resource is subject to an MTA.

EXPERIMENTAL MODELS AND SUBJECT DETAILS

Xenopus laevis

Wild-type and transgenic *Xenopus laevis* were obtained from the National *Xenopus* Resource (NXR) at Marine Biological Laboratory, Woods Hole, USA, and the European *Xenopus* Resource Centre (EXRC) at University of Portsmouth, School of Biological Sciences, UK. Frog maintenance and care was conducted according to standard procedures and based on recommendations provided by the international *Xenopus* community resource centers NXR and EXRC as well as by Xenbase (http://xenbase.org). All experiments were conducted in embryos derived from at least two different females and independent *in vitro* fertilizations.

Mice

Mice from the strain TCF/Lef1-HISTH2BB/EGFP (61Hadj/J) (Ferrer-Vaquer et al., 2010) were obtained from the Jackson Laboratories (JAX) and genotyped using the protocol deposited under https://jax.org/strain/013752. Reporter analysis was conducted on tissues derived from male and female animals and no differences were observed between the sexes. Animal care was conducted by centralized facilities and according to standard procedures.

Immortalized Human Basal Cells (BCIs)

BCIs were generated as described in Walters et al. (2013) and were provided by the Crystal laboratory. All experiments were conducted on cells derived from the same passage (passage 10). Expansion and ALI cultures of BCIs were conducted according to Walters et al. (2013) at 37°C.

Ethics Statements on Animal Experiments

This work was done in compliance with German animal protection laws and was approved under Registrier-Nr. X-18/02F and G-18/76 by the state of Baden-Württemberg, as well as with approval of University of California, Berkeley's Animal Care and Use

Committee. University of California Berkeley's assurance number is A3084-01, and is on file at the National Institutes of Health Office of Laboratory Animal Welfare.

METHOD DETAILS

Manipulation of *Xenopus* Embryos, Constructs, and In Situ Hybridization

X. laevis eggs were collected and *in vitro*-fertilized, then cultured and microinjected by standard procedures (Sive et al., 2010). Embryos were injected with Morpholino oligonucleotides (MOs, Gene Tools) and mRNAs at the four-cell stage using a PicoSpritzer setup in 1/3x Modified Frog Ringer's solution (MR) with 2.5% Ficoll PM 400 (GE Healthcare, #17-0300-50), and were transferred after injection into 1/3x MR containing Gentamycin. Drop size was calibrated to about 7–8 nL per injection.

Morpholino oligonucleotides (MOs) were obtained from Gene Tools targeting *ctnnb1.L and .S* (Heasman et al., 2000), or targeting *ΔN-tp63.L and .S* (this study), and used at doses ranging between 34 and 51ng (or 4-6pmol).

ΔN-tp63 was cloned from total cDNA into pCS107 using ΔN-tp63-f and ΔN-tp63-stop-r primers matching NCBI reference sequence XM_018261616.1. BamH1/Sal1 restriction enzymes were used for subcloning. A *gfp-ΔN-tp63* fusion construct was generated using gfp-f and gfp-r, and BamH1 restriction enzyme to fuse GFP to the N terminus of pCS107-ΔN-tp63. A hormone-inducible *gfp-ΔN-tp63-gr* fusion construct was generated using a non-stop-sequence (ΔN-tp63-nonstop-r), primers for the GR-domain (Kolm and Sive, 1995) gr-lbd-f and gr-lbd-r, and Sal1 restriction enzymes to fuse the GR domain to the C terminus of pCS107-gfp-ΔN-tp63. All sequences were verified by Sanger sequencing, and linearized with Asc1 to generate mRNAs (used at 150ng/μl) and pCS107-*ΔN-tp63* with BamH1 to generate an anti-sense probe template.

mRNAs encoding membrane-GFP or membrane-RFP or Centrin4-CFP (Antoniades et al., 2014) were used in some experiments as lineage tracers at 50 ng/μL (not shown). All mRNAs were prepared using the Ambion mMessage Machine kit using Sp6 (#AM1340).

DNAs were purified using the PureYield Midiprep kit (Promega, #A2495) and were linearized before *in vitro* synthesis of anti-sense RNA probes using T7 or Sp6 polymerase (Promega, #P2077 and #P108G), RNase Inhibitor (Promega #N251B) and Dig-labeled rNTPs (Roche, #3359247910 and 11277057001). Embryos were *in situ* hybridized according to Harland (1991), bleached after staining and imaged. Sections were made after embedding in gelatin-albumin with glutaraldehyde at 50-70 μm as described in Walentek et al. (2012).

Drug treatment of embryos started and ended at the indicated stages. DMSO (Sigma, #D2650) or ultrapure Ethanol (NeoFroxx #LC-8657.3) were added to the medium as vehicle controls. 6-Bromoindirubin-3′-oxime (BIO, Sigma-Aldrich/Merck #B1686) was used in DMSO at 75 μM (BIO low) or 150 μM (BIO high). Dexamethasone (Sigma-Aldrich/Merck #D4902) was used in Ethanol at 10 μM.

Morpholino nucleotide and cloning primer sequences:

Name	Sequence
β-catenin MO	5′-TTTCAACCGTTTCCAAAGAACCAGG −3′
ΔN-tp63 MO	5′-GATACAACATCTTTGCAGTGAGGTT-3′
ΔN-tp63-f	AAAAAAGGATCCATGTTGTATCTGGAAAACAATG
ΔN-tp63-stop-r	GTCGACTCATTCACCCTCTTCCTTAATAC
ΔN-tp63-nonstop-r	GTCGACTTCACCCTCTTCCTTAATAC
gfp-f	AAAAAAGGATCCATGGTGAGCAAGGGCGAGG AGCTGTTC
gfp-r	AAAAAAGGATCCCTTGTACAGCTCGTCCATGC CATGCCGAGAGTG
gr-lbd-f	AAAAAGTCGACCCTCTGAAAATCCTGGTAA CAAAAC
gr-lbd-r	AAAAAGTCGACCTACACTTTTGATGAAACAGAAG

(-

Generation of the Xenopus Wnt/β-catenin Signaling Reporter Line

The Wnt reporter line *Xla.Tg(WntREs:dEGFP)*^{Vlemx} was generated using the sperm nuclear transfer method as described in detail in Hirsch et al. (2002). The Wnt-responsive promoter consists of 7 copies of a TCF/LEF1 binding DNA element and a minimal TATA box and a reporter gene encoding destabilized EGFP and a polyA sequence. The transgene is flanked on both sides by two copies of the chicken HS4-core sequence (Tran et al., 2010).

RNA-Sequencing on Xenopus Mucociliary Organoids and Bioinformatics Analysis

X. laevis embryos were either injected 4x into the animal hemisphere at four-cell stage with *ΔN-tp63* MO or remained uninjected, and were cultured until st. 8. Animal caps were dissected in 1x Modified Barth's solution (MBS) and transferred to 0.5x MBS + Gentamycin

Sive et al., 2010). 10-15 organoids were collected in TRIzol (Thermo Fisher #15596026) per stage at st. 10.5 (st. 10), st. 16-19 (st. 17) and st. 24-25 (st. 25). Organoids were derived from 3 independent experiments.

500 ng total RNA per sample was used, poly-A selection and RNA-sequencing library preparation was done using non strand massively-parallel cDNA sequencing (mRNA-Seq) protocol from Illumina, the TruSeq RNA Library Preparation Kit v2, Set A (Illumina #RS-122-2301) according to manufacturer's recommendation. Quality and integrity of RNA was assessed with the Fragment Analyzer from Advanced Analytical by using the standard sensitivity RNA Analysis Kit (Advanced Analytical #DNF-471). All samples selected for sequencing exhibited an RNA integrity number over 8. For accurate quantitation of cDNA libraries, the Quanti-FluordsDNA System from Promega was used. The size of final cDNA libraries was determined using the dsDNA 905 Reagent Kit (Advanced Bioanalytical #DNF-905) exhibiting a sizing of 300 bp on average. Libraries were pooled and paired-end 100bp sequencing on a HiSeq2500 was conducted at the Transcriptome and Genome Analysis Laboratory, University of Göttingen. Sequence images were transformed with Illumina software BaseCaller to BCL files, which was demultiplexed to fastq files with bcl2fastq v2.17.1.14. Quality control was done using FastQC v0.11.5 (Andrews, 2010). "FastQC a quality-control tool for high-throughput sequence data" available at http://www.bioinformatics.babraham.ac.uk/projects/fastqc).

Sequencing generated a total of 2x 581.7 Mio reads (average 2x 32.3 Mio / library). After adaptor-trimming, paired-end reads were mapped to *Xenopus laevis* genome assembly v9.2 using RNA STAR v2.6.0b-1 (Dobin et al., 2013). featureCounts v1.6.3 (Liao et al., 2014) was used to count uniquely mapped reads per gene and statistical analysis of differential gene expression was conducted in DEseq2 v1.22.1 (Love et al., 2014). Go-term analysis was done with "humanized" versions of *Xenopus* gene names (by removing ".L" and ".S" from the name) using the GO Consortium website (http://geneontology.org). Heatmaps were generated in R v3.5.1 using ggplot2/heatmap2 v2.2.1. All bioinformatic analysis was performed on the Galaxy / Europe platform (http://usegalaxy.eu).

Air-Liquid Interface (ALI) Culture of Immortalized Human Basal Cells (BCIs)

ALI cultures of BCIs were conducted according to Walters et al. (2013) on Costar Transwell Filters (Costar #3470), coated with human Type IV Collagen (Sigma #C7521) dissolved in Acetic acid (Carl Roth #3738.4). For Basal cell expansion the BEGM Bullet Kit (Lonza #CC-3170) was used with all supplements as recommended by the manufacturer, but without the antibiotics. Instead, Penicillin-Streptomycin (0.5%, Sigma #P4333), Gentamycin sulfate (0.1%, Carl Roth, #2475.1) and Amphotericin B (0.5%, GIBCO #15290-018) were added. Differentiation of cells was conducted in DMEM:F12 (GIBCO #11330-032) with UltroserG (2%, Pall BioSphera-Science #15950-017 dissolved in sterile cell culture grade water from GIBCO #15230-071), and Penicillin-Streptomycin (0.5%, Sigma #P4333), Gentamycin sulfate (0.1%, Carl Roth, #2475.1) and Amphotericin B (0.5%, GIBCO #15290-018) for up to 28 days. Media were filtered (0.22 μm) before use. Manipulations of Wnt signaling were done by addition of human recombinant RSPO2 (R&D systems 3266-RS) or human recombinant DKK1 (R&D systems 5439-DK), which were reconstituted in sterile PBS, pH 7.4 containing 0.1% bovine serum albumin at 200ng/ml.

ALI Culture of Primary Mouse Tracheal Epithelial Cells (MTECs)

ALI cultures of MTECs were conducted according to Vladar and Brody (2013) on Costar Transwell Filters (Costar #3470), coated with rat tail Collagen (BD Biosciences #354236) in Acetic acid. Cells were isolated from TCF/Lef1-HISTH2BB/EGFP (61Hadj/J). Reagents and supplements were used as indicated in the protocol (see Key Resources Table for details). Primaria cell culture dishes (Corning #353803) were used for selection during the procedure. Cells were cultured for up to 21 days.

Quantitative RT-PCR on cDNAs from BCIs

Before total RNA extraction from BCIs, filters were washed 3x 5 min with PBS and removed from the insets using a scalpel cleaned with RNase away (MbP #7002). The RNeasy Mini Kit (QIAGEN #74104) was used, and the cells were collected in RLT buffer + β-Mercaptoethanol (10 μL / ml), vortexed for 2 min, and lysed using QIAshredder (QIAGEN #79654) columns. RNA was collected in Ultra-Pure water (Invitrogen #10977-035) and used for cDNA synthesis with iScript cDNA Synthesis Kit (Bio-Rad #1708891). qPCR-reactions were conducted using Sso Advanced Universal SYBR Green Supermix (Bio-Rad #172-5275) on a CFX Connect Real-Time System (Bio-Rad) in 96-well PCR plates (Brand #781366). Experiments were conducted in biological and technical triplicates and normalized by *GAPDH* and *ODC* expression levels. Expression levels were analyzed in Excel and graphs were generated using R. Primers and sequences can be found in Table S3.

Immunofluorescence Staining and Sample Preparation

Whole *Xenopus* embryos, were fixed at indicated stages in 4% paraformaldehyde at 4°C over-night or 2 h at room temperature, then washed 3x 15 min with PBS, 2x 30 min in PBST (0.1% Triton X-100 in PBS), and were blocked in PBST-CAS (90% PBS containing 0.1% Triton X-100, 10% CAS Blocking; ThermoFisher #00-8120) for 1h at RT. For cryo sections, embryos were equilibrated in 50% Sucrose at 4°C over-night, embedded in O.C.T. cryomedium (Tissue-Tek #25608-930), frozen at −80°C, and sectioned at 30-50 μm. Immunostaining on sections was done as for whole embryos after initial 3x 15 min washes with PBS and 15 min re-fixation in 4% paraformaldehyde at RT.

Mouse lungs were dissected, washed in ice-cold PBS several times and fixed at indicated stages in 4% paraformaldehyde at 4°C for >24 h. The tissue was then equilibrated in 50% Sucrose at 4°C over-night, embedded in O.C.T. cryomedium (Tissue-Tek #25608-930), frozen at −80°C, and sectioned at 10-14 μm. For immunostaining, sections were washed 3x 15 min with PBS and re-fixed in 4%

paraformaldehyde at RT 15 min followed by 2x 30 min washes in PBST (0.1% Triton X-100 in PBS). Samples were blocked in PBST-CAS (90% PBS containing 0.1% Triton X-100, 10% CAS Blocking) for 30 min – 1 h at RT.

MTEC and BCI cells grown in ALI culture were washed 3x 5 min with PBS before fixation in 4% paraformaldehyde at 4°C for >24 h. The culture filters were removed from the insets using a scalpel, divided into multiple parts and used for different combinations of stains. Filter parts were washed 2x 30 min in PBST (0.1% Triton X-100 in PBS) and blocked in PBST-CAS (90% PBS containing 0.1% Triton X-100, 10% CAS Blocking) for 30 min – 1 h at RT. A list of primary antibodies used in this study can be found in the Key Resources Table.

Secondary antibodies (used at 1:250): AlexaFluor 555-labeled goat anti-mouse antibody (Molecular Probes #A21422), AlexaFluor 488-labeled goat anti-rabbit antibody (Molecular Probes #R37116), AlexaFluor 488-labeled donkey anti-mouse antibody (Molecular Probes #R37114), AlexaFluor 405-labeled goat anti-mouse antibody (Molecular Probes #A-31553). All antibodies were applied in 100% CAS Blocking (ThermoFisher #00-8120) over night at 4°C or 2 h at RT (for secondary antibodies). DAPI was used to label nuclei (applied for 30 min. at room temperature, 1:100 in PBSt; Molecular Probes #D1306) in *Xenopus*. ProLong Gold Antifade Mountant with DAPI (Molecular Probes #P36931) was used to label nuclei in mouse and human samples. Actin was stained by incubation (30-120 min at room temperature) with AlexaFluor 488- or 647-labeled Phalloidin (1:40 in PBSt; Molecular Probes #A12379 and #A22287), mucus-like compounds in *Xenopus* were stained by incubation (overnight at 4°C) with AlexaFluor 647-labeled PNA (1:1000 in PBSt; Molecular Probes #L32460).

Confocal Imaging, Image Processing, and Analysis

Confocal imaging was conducted using a Zeiss LSM700 or Zeiss LSM880 and Zeiss Zen software. Wnt reporter sections from *Xenopus* and mice were imaged using tile-scans and images were reconstructed in ImageJ or Adobe Photoshop. Confocal images were adjusted for channel brightness/contrast and Z stack projections or orthogonal sections were generated using ImageJ. A detailed protocol for quantification of *Xenopus* epidermal cell types was published (Walentek, 2018). Images of embryos after *in situ* hybridization and corresponding sections were imaged using an AxioZoom setup or AxioImager.Z1, and images were adjusted for color balance, brightness, and contrast using Adobe Photoshop. Measurement of *ΔN-tp63* domain thickness in *Xenopus* was done in ImageJ using the NeuronJ plugin.

QUANTIFICATION AND STATISTICAL ANALYSIS

Statistical Evaluation

Stacked bar graphs were generated in Microsoft Excel, boxplots and heatmaps were generated in R (the line represents the median; 50% of values are represented by the box; 95% of values are represented within whiskers; values beyond 95% are depicted as outliers). Statistical evaluation of experimental data was performed using chi-square tests (http://www.physics.csbsju.edu/stats/contingency.html), Wilcoxon sum of ranks (Mann-Whitney) tests (https://astatsa.com/WilcoxonTest/), or Student's t test (http://www.physics.csbsju.edu/stats/t-test.html) as indicated in figure legends.

Sample Size and Analysis

Sample sizes for all experiments were chosen based on previous experience and used embryos derived from at least two different females in *Xenopus*. Analysis of mouse Wnt-reporter was conducted in samples from N > 3 animals. No randomization or blinding was applied.

Use of Shared Controls

For parts of cell type quantification in *Xenopus* and BCIs, and qPCR experiments in BCIs shared controls or other conditions were used in multiple figures/graphs. Therefore, a detailed log of manipulation experiments in *Xenopus* and BCIs is provided in Table S2. It contains information on experiment number, species/model, type of experiment, conditions, number of specimens, and in which figure/graph the data were used throughout the manuscript.

DATA AND SOFTWARE AVAILABILITY

RNA-seq data have been deposited in the NCBI Gene expression Omnibus (GEO) database under the ID: GEO: GSE130448 (https://www.ncbi.nlm.nih.gov/geo/query/acc.cgi?acc=GSE130448).